




$O(N)$ smectic σ model

Tzu-Chi Hsieh  and Leo Radzihovsky 

Department of Physics and Center for Theory of Quantum Matter, University of Colorado, Boulder, Colorado 80309, USA

 (Received 30 October 2023; accepted 22 November 2023; published 18 December 2023)

A unidirectional “density” wave order in an otherwise *isotropic* environment is guaranteed to display a smecticlike Goldstone mode. Examples of such soft states include conventional smectic liquid crystals, putative Fulde-Ferrell-Larkin-Ovchinnikov superfluids, and helical states of frustrated bosons and spins. Here we develop generalized spin-smectic σ -models that break $O(N)$ internal symmetry in addition to the d -dimensional rotational and uniaxial translational symmetries. We explore long-wavelength properties of such strongly fluctuating states, show that they are characterized by a “double-power-law” static structure peak, and analyze their asymptotic symmetry-reduced crossover to conventional low-energy modes. We also present the associated Ginzburg-Landau theory, describing the phase transition into such spin-smectic states, and we discuss experimental realization of such models.

DOI: [10.1103/PhysRevB.108.224423](https://doi.org/10.1103/PhysRevB.108.224423)

I. INTRODUCTION

A. Background and motivation

There are a number of systems in nature that spontaneously undergo transitions to a variety of “density” [1] wave states, characterized by a periodic modulation. Such systems range from a large variety of charge and spin density waves, e.g., antiferromagnetic insulators in cuprates [2], charge density waves in NbSe₃ [3], and Wigner crystal [4], to the putative pair-density wave superconductors [5]. Generically, in an orientationally ordered environment of a crystal, the low-energy nonlinear σ -model ($n\sigma m$) description of the corresponding Goldstone modes is given by their linear gradient elasticity at weak coupling controlled by a Gaussian fixed point, and it is thus quite well-understood [2,6–10].

In contrast to these systems, there exists a qualitatively distinct class of phases of matter, where a unidirectional density-wave order (characterized by a spontaneously oriented wave vector \mathbf{q}_0) takes place in an isotropic environment, and thus, in addition to translational and internal symmetries, also spontaneously breaks *spatial rotational* symmetry. We expect such states to be described by a “soft”—higher gradient— $n\sigma m$ that is qualitatively distinct from their crystalline counterparts. The derivation and study of such models is the focus of the present work.

The simplest realization of such states is the extensively studied conventional smectic liquid crystals [11] characterized by a periodic *scalar* number-density, described by a fully rotationally invariant soft nonlinear elastic model [12,13]. In the presence of thermal and quantum fluctuations or quenched disorder [14–16], the corresponding scalar phonon (denoted as u) fluctuations are qualitatively enhanced (e.g., for spatial dimension $d \leq 3$, thermal u_{rms} grows with system size, diverging in the thermodynamic limit) and lead to the importance of the nonlinear elasticity [12], resulting in a tuning-free critical smectic phase described by universal exponents [17].

In this paper, we consider a generalization of such a scalar smectic to “spin” (nonscalar) density, $\vec{S}(\mathbf{x})$, that transforms

nontrivially under $O(N)$ -spin rotational symmetry. Such a state, that we dub “spin-smectic,” is characterized by an internal flavor degree of freedom, and it exhibits a spontaneous uniaxial spatial modulation in $\vec{S}(\mathbf{x})$ along \mathbf{q}_0 . It thereby spontaneously breaks the $O(N)$ -internal spin symmetry, and the underlying spatial $O(d)$ -rotational and $T(d)$ -translational symmetries.

Our study of such spin-smectics is motivated by a number of physical realizations of unidirectional orders, that include (i) $O(N=1)$: conventional smectic liquid crystal [11], and quantum Hall striped states of a two-dimensional electron gas at half-filled high Landau levels [18–23]; (ii) $O(N=2)$: cholesteric liquid crystal [24], spin-orbit coupled and dipolar Bose condensates [25,26], putative Fulde-Ferrell-Larkin-Ovchinnikov (FFLO) paired superfluids [27,28] in imbalanced degenerate atomic gases [29,30], a p -wave resonant Bose gas [31,32], and helical states of frustrated bosons [33]; (iii) $O(N=3)$: helimagnets of frustrated spin systems [34–36], as realized in spinel materials, e.g., CoAl₂O₄ [37,38] and MnSc₂S₄ [39], van der Waals honeycomb magnets, e.g., FeCl₃ [40], and a stretched diamond lattice, e.g., LiYbO₂ [41]. For long-wavelength $2\pi/q_0 \gg a$ (lattice constant) spin-density modulation, even in the crystalline realizations with spin-orbit interactions above, we expect the spin-smectics to emerge in a broad range of intermediate scales from an *approximate* rotationally symmetric state, even if asymptotically crossing over to more conventional ordered states.

B. Frustrated J_1 - J_2 spin model

Before we summarize our main findings, we discuss the frustrated J_1 - J_2 lattice model, studied at a microscopic level in Refs. [35,36]. The long-scale phenomenology that emerges from this model motivates our current study.

Its Hamiltonian is given by

$$H = J_1 \sum_{\langle ij \rangle} \vec{S}_i \cdot \vec{S}_j + J_2 \sum_{\langle\langle ij \rangle\rangle} \vec{S}_i \cdot \vec{S}_j, \quad (1)$$

where \vec{S}_i is an N -component spin on site i (with $N = 1, 2, 3$, respectively, corresponding to the Ising, XY , and Heisenberg models), and $\langle ij \rangle$ and $\langle\langle ij \rangle\rangle$ denote the nearest-neighbor (NN) and next-nearest-neighbor (NNN) pairs of sites. The frustration of the system is then induced by the antiferromagnetic NNN interactions, $J_2 > 0$, while the sign of the NN exchange interactions is not important (as it is nonfrustrating and can be changed by a bipartite transformation), but for concreteness and convenience we take it to be $J_1 > 0$. Then, the spin frustration is characterized by the ratio, $J_2/J_1 > 0$. In the classical $S = \infty$ limit, the model (1) exhibits ground-state degeneracy. Taking the diamond-lattice antiferromagnets (as realized in AB_2X_4 compounds, with A a magnetic ion living on a diamond lattice and B living on a pyrochlore lattice, studied by Bergman *et al.* [35]) for example, for weak frustration, $0 < J_2/J_1 < 1/8$, the ground state is the Néel state. For intermediate frustration, $1/8 < J_2/J_1 < 1/4$, the ground state is an incommensurate helical spin-density wave that is degenerate with respect to orientation of the ordering wave vector \mathbf{q}_0 on the so-called spiral codimension 1 surface around the Γ point. For $1/4 < J_2/J_1$, the spiral surface exhibits open topology along the (111) axis, and in the limit $J_2/J_1 \rightarrow \infty$, it collapses into one-dimensional lines that correspond to the nearest-neighbor-coupled face-centered cubic antiferromagnet.

As a consequence of the large classical ground-state degeneracy, the ordering temperature, T_c , is small relative to the Curie-Weiss exchange scale, Θ_{CW} [42]. For example, spinel compounds like CoAl_2O_4 [37,38] and MnSc_2S_4 [39] have $|\Theta_{CW}| > 10 - 20T_c$ and $|\Theta_{CW}| \approx 10T_c$, respectively. This is considered as empirical signatures of highly frustrated magnets. As an aside, this then leads to a broad regime of spiral classical spin liquid for temperatures $T_c < T < |\Theta_{CW}|$, where the system thermally explores many different low-energy configurations on the spiral surface and thereby exhibits anomalous physical properties. This is in contrast with an even more exotic quantum spin liquid that survives down to zero temperature [43].

At low temperatures, $T < T_c$, the ordering of such magnets is associated with the lifting of the spiral surface degeneracy that is sensitive to the degeneracy-breaking perturbations like spin-orbit and crystalline symmetry breaking anisotropies. In the absence of such perturbations, the spiral surface degeneracy is lifted via quantum and thermal fluctuations in the free energy, which select a set of wave vectors (whose magnitude is given by the radius of spiral surface, q_0) of the ordered states that one expects to be along the crystalline symmetry axes—the so-called order-by-disorder [44,45]. The resulting low-temperature ordered phases range from the nematic [36] to a variety of spin-density-wave states at specific wave vector [35]. The ordering of the latter self-consistently introduces a stabilizing stiffness of a conventional $n\sigma m$ and thereby determines other physical observables such as the specific heat and structure factor [33,35]. As a result, the fluctuation-generated stiffness is small, subdominant to the higher-order gradient elasticity over a large regime (set by order-by-disorder scale), within which the system exhibits the softer (than conventional spin-density-wave states) smecticlike elasticity [33]. Our goal here is to study the universal low-energy description and phenomenology of such soft, unidirectionally ordered spin-

TABLE I. Goldstone mode number and type in the coplanar and collinear $O(N)$ spin-smectics for different number N of spin components. N_{GM} is the number of the Goldstone modes. “Sm”, “XY,” and “ $O(N)$ ” stand for smectic, XY , and $O(N)$ Goldstone mode models, respectively.

	Coplanar	Collinear
N_{GM}	$2N - 3$	N
$N = 1$	N/A	Sm
$N = 2$	Sm	Sm + XY
$N \geq 3$	soft $n\sigma m$, (2)	Sm + $O(N)$, (4)

density-wave states, which we refer to as spin-smectics. To this end, in this paper we primarily focus on an isotropic (i.e., neglecting the order-by-disorder and lattice symmetry breaking effects) field theory controlled by the ordering on the spiral momentum surface.

C. Results

1. Coplanar smectic σ -model

Motivated by the above physical systems and the frustrated J_1 - J_2 Heisenberg model [35,36], generalized to N spin components, our key result (summarized for different cases of interest in Table I) is the derivation of the $O(N)$ smectic σ -model for an N -component orthonormal $\hat{n}(\mathbf{x}) - \hat{m}(\mathbf{x})$ diad, described by the Hamiltonian density

$$\mathcal{H}_{\text{coplanar}}[\hat{n}, \hat{m}] = J|\nabla^2 \hat{\psi}|^2 + 2iq_0 \partial_{\parallel} |\hat{\psi}|^2 + \kappa(\nabla \hat{L})^2. \quad (2)$$

It describes the nonlinear Goldstone modes of the $N \geq 3$ coplanar spiral state at a wave vector \mathbf{q}_0 [see Fig. 1(a)]. In the above, we defined components of spin fluctuations $\hat{L}_{\alpha\beta} = n_{\alpha}m_{\beta} - n_{\beta}m_{\alpha}$ transverse to the spiral plane \hat{n} - \hat{m} and the complex vector $\hat{\psi} = (\hat{n} + i\hat{m})/\sqrt{2}$. For simplicity of presentation here, we neglected inessential (quantitative) anisotropy in κ , discussed in the main body of the paper. Throughout this paper, we use the subscripts \parallel ($\equiv \hat{\mathbf{q}}$) and \perp to denote the axes parallel and perpendicular to \mathbf{q}_0 , respectively. The J modulus describes the “soft” Goldstone-mode elasticity for the fluctuations in the \hat{n} - \hat{m} plane, which for weak excitations reduces to the standard smectic form, (33), and also introduces κ_{\parallel} stiffness for \hat{L} . The κ terms give linear-gradient elasticity for the out-of- \hat{n} - \hat{m} -plane fluctuations. We find that $B, K, \kappa_{\parallel} \propto S_0^2$, $\kappa_{\perp} \propto S_0^4$, predicting a divergent anisotropy near the critical point, where $S_0 \rightarrow 0$.

For the special case of $N = 3$, the spin-smectic σ -model in (2) reduces to

$$\begin{aligned} \mathcal{H}_{\text{coplanar}} &= J|\nabla^2 \hat{\psi}|^2 + 2iq_0 \partial_{\parallel} |\hat{\psi}|^2 + \kappa(\nabla \hat{L})^2 \\ &= \frac{J}{2}(\nabla^2 \hat{n} - 2q_0 \partial_{\parallel} \hat{m})^2 + \frac{J}{2}(\nabla^2 \hat{m} + 2q_0 \partial_{\parallel} \hat{n})^2 \\ &\quad + \kappa(\nabla \hat{L})^2, \end{aligned} \quad (3)$$

where the complex 3-vector $\hat{\psi} = (\hat{n} + i\hat{m})/\sqrt{2}$, defining an orthonormal triad $\hat{n} \times \hat{m} = \hat{\ell}$.

Easy-plane (XY) anisotropy $-(\hat{\ell} \cdot \hat{c})^2$ locks $\hat{\ell}$ along the anisotropy axis \hat{c} , reducing the model to an $N = 2$ conven-

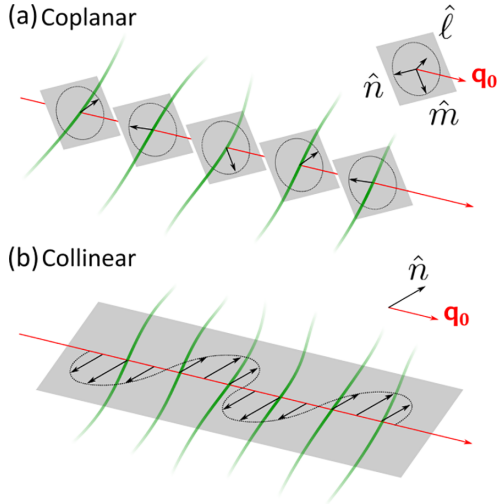


FIG. 1. A schematic of $N = 3$ (a) coplanar and (b) collinear spin-smectics. The black and red arrows denote the spins $\vec{S}(\mathbf{x})$ and the spiral wave vector \mathbf{q}_0 , respectively. The green (online) curves denote the spin-smectic phase fronts of constant spin magnitude and orientation, with the nearby fronts separated by an arbitrarily chosen phase of $2\pi/3$. Upper right insets: The coplanar state is described by an orthonormal triad $\hat{n}(\mathbf{x}), \hat{m}(\mathbf{x}), \hat{\ell}(\mathbf{x})$, with \hat{n} and \hat{m} defining the spin $\vec{S}(\mathbf{x})$ plane that in the absence of spin-orbit interaction (that is our focus here) is decoupled from \mathbf{q}_0 . The collinear state is characterized by a unit vector $\hat{n}(\mathbf{x})$ that denotes the axis of the collinear spin-density wave.

tional smectic σ -model, of, e.g., cholesteric and Fulde-Ferrell states for ϕ with $\hat{n} = (\cos \phi, \sin \phi)$.

2. Collinear smectic σ -model

For *collinear* spiral states [see Fig. 1(b)], the low-energy Goldstone modes are a smectic-like pseudophonon $u(\mathbf{x})$ corresponding to the spin-density-wave phase and a unit vector $\hat{n}(\mathbf{x})$ that describes local spin orientation. These are characterized by a Hamiltonian density

$$\mathcal{H}_{\text{collinear}}[u, \hat{n}] = Bu_{qq}^2 + K(\nabla^2 u)^2 + \kappa(\nabla \hat{n})^2, \quad (4)$$

where $u_{qq} = \partial_q u + (\nabla u)^2/2$ is the rotationally invariant strain tensor. In the presence of easy-axis anisotropy $g(\hat{n} \cdot \hat{c})^2$ common to magnetic crystalline materials, when $g < 0$, the spin orientation \hat{n} freezes out, leading to a low-energy $N = 1$ smectic σ -model described by a single smectic phonon derived in Sec. II A. When $g > 0$, the spin orientation \hat{n} is locked perpendicular to \hat{c} , resulting in an $N = 2$ collinear smectic, such as the Larkin-Ovchinnikov state.

3. Thermal fluctuations and structure factor

Focusing on the physical case, $N = d = 3$, we show that both the coplanar and collinear states are described by a smectic phonon and two XY Goldstone modes at the harmonic level, i.e., at the Gaussian fixed point, neglecting effects of nonlinearities that may lead to a crossover to a nontrivial spin-smectic fixed point, thereby modifying these predictions at long scales. Accordingly, they both exhibit quasi-long-range and long-range orders in their spin-density modulation and

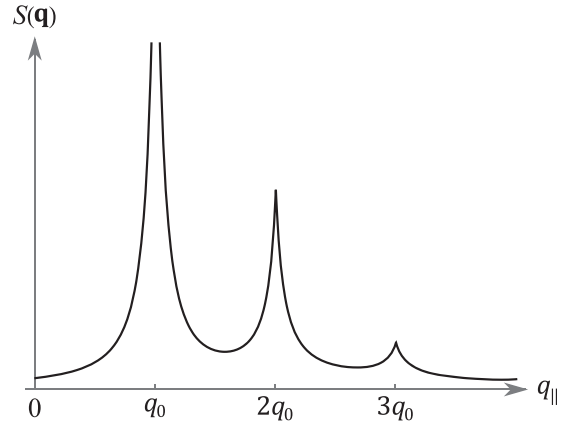


FIG. 2. Schematic plot of the structure factor $S(\mathbf{q})$ for the $O(3)$ collinear and coplanar spin-smectic states that display double-power-law quasi-Bragg (as opposed to single-power-law and δ -function) peaks at $\mathbf{q} = \pm n\mathbf{q}_0$.

spin orientation orders, respectively. As illustrated in Fig. 2, this then leads in 3D to anisotropic double-power-law peaks in their static spin structure factor at $\pm n\mathbf{q}_0$ ($n = 1, 2, 3, \dots$) [see Eq. (111) for a more detailed form],

$$S(\mathbf{q}) \approx \sum_n P_n(\mathbf{q} - n\mathbf{q}_0) + \sum_n P_n(\mathbf{q} + n\mathbf{q}_0), \quad (5)$$

where ($a = 1$)

$$P_n(\mathbf{k}_\perp = 0, k_\parallel) \sim \frac{1}{|k_\parallel|^{2-\eta_n}} + \frac{T}{\kappa} \frac{1}{|k_\parallel|^{1-\eta_n+\frac{1}{1+2\eta_n}}} \quad (6)$$

with the positive temperature-dependent exponent $\eta_n = n^2 q_0^2 T / 16\pi \sqrt{BK}$. In the above, the first term is the leading (narrower) smectic Goldstone mode contribution of the power-law peak, while the second term is the subleading (broader) contribution from the XY Goldstone mode fluctuations, with the prediction valid at small T/κ , expected to become important as this ratio becomes of order 1 or larger.

We discuss the effects of various symmetry-breaking perturbations that exist in real materials, including the lattice anisotropy and spin-orbit coupling. The former breaks the $O(d = 3)$ spatial rotational symmetry, and thereby leads to a crossover for the smectic phonon mode to XY correlation (see Fig. 5). This results in true Bragg peaks (δ functions), as in conventional long-range-ordered states, but may keep the power-law tail at intermediate scales if the symmetry-breaking perturbation is weak. On the other hand, the spin-orbit coupling, as, e.g., Dzyaloshinskii-Moriya (DM) interaction in a helimagnet (or a chiral twist term in a cholesteric), breaks $O(N = 3) \times O(d = 3)$ symmetries down to the diagonal subgroup. For the coplanar state, this locks the orientation of $\hat{\ell}$ perpendicular to \mathbf{q}_0 , and thereby freezes out the two XY Goldstone modes, resulting in a single-power-law peak with the second term in (6) suppressed.

4. Transition into the spin-smectic: $O(N)$ de Gennes model

To describe the criticality associated with the phase transition into these spin-smectic states, illustrated in Fig. 3, we also derive a generalized $O(N)$ de Gennes model [11], with

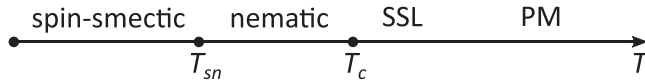


FIG. 3. Schematic phase diagram for the frustrated J_1 - J_2 Heisenberg model with a low-temperature spin-density wave that also breaks (at intermediate scales for a lattice system with weak spin-orbit coupling) translational and spatial rotational symmetries, thereby exhibiting what we dub a “spin-smectic.” We expect it to melt at T_{sn} into an orientationally ordered spin-nematic (both in spin, $\langle S_\alpha S_\beta \rangle \approx \delta_{\alpha\beta}$, and coordinate, $\langle q_i q_j \rangle \approx \delta_{ij}$, spaces). The spin-nematic then disordered at T_c into a spiral spin liquid (SSL) (characterized by a short-range smectic order) that then crosses over into a paramagnetic state (PM).

Hamiltonian density given by

$$\mathcal{H}_{GL} = r|\vec{\psi}|^2 + v_1|\vec{\psi}|^4 + \frac{v_2}{2}|\vec{\psi} \cdot \vec{\psi}|^2 + \frac{J}{2}|(i\nabla - q_0\delta\mathbf{N})\vec{\psi}|^2 + K_s(\nabla \cdot \delta\mathbf{N})^2 + K_b(\nabla \times \delta\mathbf{N})^2, \quad (7)$$

where the complex vector $\vec{\psi} = \vec{n} + i\vec{m}$ (\vec{n} and \vec{m} are independent N -vectors, physical cases corresponding to $N = 1, 2, 3$) describes the spin-density-wave order parameter, and $\delta\mathbf{N} = \mathbf{N} - \hat{\mathbf{q}}$, with \mathbf{N} a *spatial* unit vector that describes the translationally invariant nematic liquid that spin-smectic melts into for $r > 0$. This Ginzburg-Landau theory, which we dub the $O(N)$ spin-de Gennes model, at low temperatures for $r < 0$ predicts the collinear ($v_2 < 0$) and coplanar ($v_2 > 0$) states discussed above.

5. Quantum dynamics

By including the Wess-Zumino-Witten Berry phase, which encodes the spin precessional dynamics and corresponding spin commutation relations, we supplement the above $O(N)$ classical smectic σ -models with quantum dynamics in the spin-coherent path integral. For an $N = 3$ coplanar state we find that Berry phase action for the smectic σ -model is given by a

$$S_B = \gamma \int_{\mathbf{x}, t} [(\partial_t \hat{n})^2 + (\partial_t \hat{m})^2 + 2(\hat{m} \cdot \partial_t \hat{n})^2], \quad (8)$$

where γ is the uniform ferromagnetic susceptibility in the coplanar phase.

The remainder of the paper is organized as follows. In Sec. II, we derive the continuum field theory of the lattice model (1) with generalized $O(N)$ spin symmetry and the underlying spatial $O(d)$ rotational and $T(d)$ translational symmetries. It gives our key result, a new class of “soft” $O(N) \times O(d)$ σ -models that describe the universal long-wavelength properties of spin-smectics. We show that these reduce to the fully *nonlinear* Goldstone-mode field theories for the conventional smectic liquid crystals ($N = 1$), the putative FFLO paired superfluids in imbalanced degenerate atomic gases ($N = 2$), and a new class of soft-spin-density waves ($N \geq 3$), among other physical realizations. In Sec. III, we analyze the spin-smectic in the presence of weak thermal fluctuations, assess its stability, and compute its correlation functions, focusing on the structure factor that exhibits crossovers across

a range of length scales. In Sec. IV, we introduce a complementary Ginzburg-Landau model that gives spin-smectic as its ordered state and describes the transition from the orientationally ordered to the spin-smectic states. In Sec. V, starting with the WZW term, we derive the quantum dynamics for the $O(N)$ spin-smectic σ -model. We conclude in Sec. VI with a summary of our results and a discussion of open directions.

II. FIELD THEORY OF $O(N)$ SMECTICS

The key feature of the frustrated lattice model, (1), is its degenerate ground-state manifold (neglecting order-from-disorder effects), defined by a spiral surface $\varepsilon(\mathbf{q}) = \text{const}$, where \mathbf{q} is the wave vector of the spin spiral state. Motivated by this class of models and corresponding experimental realizations of frustrated helimagnets [37–41], we develop the field theory of low-energy excitations of helical states that emerge from an *isotropic* spiral surface, $|\mathbf{q}| = q_0$, neglecting spin-orbit coupling (SOC) and rotational-symmetry-breaking lattice effects. To this end, we develop an $O(N)$ Goldstone-mode σ -model by starting with an N -component spin \vec{S} model with Hamiltonian density (throughout this paper, we employ the Einstein convention, where repeated indices are implicitly summed over),

$$\mathcal{H} = \frac{J}{2}[(\nabla^2 \vec{S})^2 - 2\bar{q}_0^2(\nabla \vec{S})^2] + \frac{r}{2}\vec{S}^2 + \lambda_1 \vec{S}^4 + \lambda_2(\vec{S} \times \nabla \vec{S})^2 + \lambda_3(\partial_i \vec{S} \cdot \partial_j \vec{S})^2 + \dots, \quad (9)$$

that encodes the coplanar and collinear spiral states on an $O(d)$ hyperspherical spiral surface, $\varepsilon(|\mathbf{q}|) = (q^2 - q_0^2)^2 = \text{const}$, that can be derived from the microscopic Hamiltonian (1). We note that the Hamiltonian (9) respects $O(d) \times O(N)$ -rotational [and $T(d)$ -translational with d the spatial dimension] symmetry, neglecting any SOC, i.e., forbidding the inner product between the spatial (∇) and “spin” (\vec{S}) degrees of freedom.

Driven by the J term, that for $r < 0$ clearly exhibits a nonzero momentum $|\mathbf{q}| = \bar{q}_0$ spin condensation on an $O(d)$ -symmetric spiral surface [46], we consider (as we will show, most strongly fluctuating) unidirectional, single \mathbf{q} spin states [47]

$$\begin{aligned} \vec{S}(\mathbf{x}) &= \vec{n}(\mathbf{x}) \cos(\mathbf{q} \cdot \mathbf{x}) - \vec{m}(\mathbf{x}) \sin(\mathbf{q} \cdot \mathbf{x}) \\ &= \text{Re}[\vec{\psi}(\mathbf{x})e^{i\mathbf{q} \cdot \mathbf{x}}], \end{aligned} \quad (10)$$

where \vec{n} and \vec{m} are N -component real vector fields, that can be compactly written as a complex N -vector field

$$\vec{\psi} = \vec{n} + i\vec{m}, \quad (11)$$

with $2N$ degrees of freedom.

The remaining quadratic and quartic terms in (9) for $r < 0$ encode Landau ordering and determine the amplitude of the spin-density-wave spiral. We note that in contrast to conventional Landau theories, here the ordering is at a nonzero wave vector, with \vec{S} condensing at a nonzero momentum $|\mathbf{q}| = q_0$. Therefore, the higher derivative $\lambda_{2,3}$ terms play an important role, as they constitute the lowest-order form needed for a generic Goldstone-mode description of the spin-smectic σ -model [48]. As we will show, the $\lambda_{2,3}$ in (9) are crucial for the stabilization of the $N \geq 2$ spin-density waves.

With the ansatz (10), the mean-field (constant part, after dropping the fast-oscillating contributions, that on spatial integration average out to zero) energy density is given by

$$\mathcal{H}_{\text{Landau}} = \frac{\tilde{r}}{4} |\vec{\psi}|^2 + \frac{v_1}{4} |\vec{\psi}|^4 + \frac{v_2}{8} |\vec{\psi} \cdot \vec{\psi}|^2, \quad (12)$$

where the zeroth-order couplings (corrected by fluctuations) are given by

$$\begin{aligned} \tilde{r} &= Jq^4 - 2Jq^2\bar{q}_0^2 + r, \\ v_1 &= \lambda_1 + \lambda_2q^2 + \lambda_3q^4, \\ v_2 &= \lambda_1 - 2\lambda_2q^2 + \lambda_3q^4. \end{aligned} \quad (13)$$

At low temperatures, $\tilde{r} < 0$ (and $v_1 > 0$), the spin-density wave is ordered and can be parametrized as

$$\vec{\psi} = S_0(\hat{n} \cos \chi + i\hat{m} \sin \chi), \quad (14)$$

where $S_0 = |\vec{\psi}|$ and χ are, respectively, the overall and relative amplitudes of order parameters \hat{n} and \hat{m} . The (mean-field) magnitude of the ordering wave vector \mathbf{q} is then determined by minimizing the Landau free energy (12), with direction chosen spontaneously. For $\lambda_2, \lambda_3 \ll \lambda_1$ we find

$$|\mathbf{q}| \equiv q_0 \approx \bar{q}_0. \quad (15)$$

It is straightforward to see that the Landau theory (12) predicts two qualitatively distinct spin-density waves. With the parametrization (14), the v_2 quartic interaction can be written as

$$\begin{aligned} |\vec{\psi} \cdot \vec{\psi}|^2 &= (n^2 - m^2)^2 + 4(\hat{n} \cdot \hat{m})^2 \\ &= S_0^4 \cos^2(2\chi) + S_0^4 \sin^2(2\chi)(\hat{n} \cdot \hat{m})^2. \end{aligned} \quad (16)$$

For $v_2 < 0$ (or $N = 1$), it is clearly minimized by

$$\hat{n} \parallel \hat{m} \quad (18)$$

with arbitrary phase, χ . This allows us to rewrite the order parameter as

$$\vec{\psi}_{\text{collinear}} = S_0 \hat{n} e^{i(\mathbf{q}_0 \cdot \mathbf{x} + \chi)}, \quad (19)$$

where the minimization of (12) then gives

$$S_0 = \sqrt{\frac{|\tilde{r}|}{2v_1 + v_2}}. \quad (20)$$

The resulting collinear spin-density wave (10) is then given by oscillatory magnitude,

$$S_{\text{collinear}}^2 = S_0^2 \cos^2(\mathbf{q}_0 \cdot \mathbf{x} + \chi). \quad (21)$$

In contrast, for $v_2 > 0$ (and $N > 1$), minimization of (17) then gives

$$\hat{n} \perp \hat{m}, \quad \chi = \pi/4 + n\pi, \quad (22)$$

where n is an arbitrary integer. This gives a coplanar, i.e., helical spin-density-wave state characterized by the order parameter

$$\vec{\psi}_{\text{coplanar}} = \frac{S_0}{\sqrt{2}}(\hat{n} + i\hat{m}), \quad (23)$$

with a constant magnitude

$$\begin{aligned} S_{\text{coplanar}}^2 &= n^2 \cos^2(\mathbf{q}_0 \cdot \mathbf{x}) + m^2 \sin^2(\mathbf{q}_0 \cdot \mathbf{x}) \\ &= S_0^2, \end{aligned} \quad (24)$$

given by

$$S_0 = \sqrt{\frac{|\tilde{r}|}{2v_1}}. \quad (25)$$

Importantly, because of the absence of SOC, both the collinear and coplanar states have decoupled spin orientation and wave vector \mathbf{q}_0 , particularly distinguishing the coplanar state from the helical state of a DM helimagnet and a cholesteric state of a chiral liquid crystal.

Based on the above analysis, below we first derive σ -models for the cases of $N = 1, 2$, which, as we will show, correspond to the familiar ordered states of a conventional smectic and the putative Fulde-Ferrell-Larkin-Ovchinnikov (FFLO) superfluids, respectively. We then study the $N = 3$ case (and its generalization to larger N), corresponding to collinear and coplanar spin-density waves, described by two distinct ‘‘soft’’ $O(3)$ nonlinear smectic σ -models. These are relevant to the ordered states of ‘‘codimension 1’’ frustrated magnetic systems reviewed in Sec. IB.

A. $N = 1$: Conventional smectic

We begin with the simplest case of $N = 1$, corresponding to a scalar number density ρ , that according to field theory (9) condenses into a *scalar*-density wave,

$$\begin{aligned} \rho(\mathbf{x}) &= \text{Re}[\psi(\mathbf{x})e^{i\mathbf{q} \cdot \mathbf{x}}] \\ &= |\psi| \cos[\mathbf{q} \cdot \mathbf{x} + q\mathbf{u}(\mathbf{x})], \end{aligned} \quad (26)$$

where $\psi = |\psi|e^{i\mathbf{q} \cdot \mathbf{x}}$, with smectic amplitude $|\psi|$ and $\mathbf{u}(\mathbf{x})$ the phonon Goldstone mode, corresponding to the displacement along \mathbf{q} , familiar from conventional smectic liquid crystals. In our generalized formulation, this $N = 1$ state corresponds to a necessarily collinear case, with one-component ‘‘vectors’’ $n \parallel m$, parametrized by $n = \rho \cos(qu)$ and $m = \rho \sin(qu)$.

At low temperatures in the ordered smectic state, the amplitude $|\psi|$ is well approximated by a mean-field value

$$\rho_0 = \sqrt{n^2 + m^2} = \sqrt{-\tilde{r}/(2v_1 + v_2)}, \quad (27)$$

with only small gapped fluctuations. Thus, with the ansatz (26) and its derivatives,

$$\begin{aligned} \nabla \rho &= \rho_0 \text{Re}[i(\mathbf{q} + q\nabla \mathbf{u})e^{i\mathbf{q} \cdot \mathbf{x} + iqu}], \\ \nabla^2 \rho &= \rho_0 \text{Re}[-(\mathbf{q} + q\nabla \mathbf{u})^2 + iq\nabla^2 \mathbf{u}]e^{i\mathbf{q} \cdot \mathbf{x} + iqu}, \end{aligned} \quad (28)$$

the model (9) (neglecting λ_2 and λ_3 , which are unimportant for $N = 1$) reduces to the familiar nonlinear smectic Goldstone-mode elasticity,

$$\begin{aligned} \mathcal{H} &= \frac{1}{4}J\rho_0^2[(\mathbf{q} + q\nabla \mathbf{u})^4 + q^2(\nabla^2 \mathbf{u})^2 - 2\bar{q}_0^2(\mathbf{q} + q\nabla \mathbf{u})^2] \\ &\quad + \frac{1}{4}r\rho_0^2 + \frac{3}{8}\lambda_1\rho_0^4 + \dots \\ &= a(q^2 - \bar{q}_0^2)u_{qq} + Bu_{qq}^2 + K(\nabla^2 u)^2 + E(\mathbf{q}), \end{aligned} \quad (29)$$

where in the first equality we dropped fast oscillating pieces that average away after spatial integration of the energy den-

sity. Above, the rotationally invariant strain tensor is

$$u_{qq} = \hat{\mathbf{q}} \cdot \nabla u + (\nabla u)^2/2 \quad (30)$$

and two independent elastic constants B and K , at zeroth order [i.e., model (9)-dependent] are given by

$$a = 4K = J\rho_0^2 q^2, \quad B = J\rho_0^2 q^4. \quad (31)$$

The minimization of the constant part of \mathcal{H} ,

$$E(\mathbf{q}) = \frac{1}{4}\rho_0^2(Jq^4 - 2Jq^2\bar{q}_0^2 + r) + \frac{3}{8}\rho_0^4\lambda_1, \quad (32)$$

over ρ_0 and q , gives $|\mathbf{q}| = \bar{q}_0$, which ensures the vanishing of the coefficient of the linear in the strain u_{qq} term, and thereby guarantees the stability of the smectic state. We note that with the inclusion of fluctuations, the optimum wave vector gets corrected, i.e., $|\mathbf{q}| = q_0 \neq \bar{q}_0$, so as to eliminate the linear in u_{qq} contribution order by order (akin to what is done with the order parameter ρ_0), which amounts to ensuring that the expansion in the nonlinear strain u_{qq} is done around the correct (fluctuation-corrected) ground state. With this, by choosing $\mathbf{q} = q_0\hat{\mathbf{z}}$, we then recover the familiar nonlinear elastic, fully rotationally invariant smectic Goldstone-mode σ -model,

$$\mathcal{H}_{\text{sm}} = Bu_{zz}^2 + K(\nabla^2 u)^2. \quad (33)$$

We observe that the emergence of smectic elasticity (33) is expected, based on spatial rotational symmetry encoded in (9), that requires a fully rotationally invariant nonlinear strain tensor u_{zz} . To see this, we note that the global rotation of the undistorted $u = 0$ smectic state is characterized by a rotation of \mathbf{q}_0 ,

$$q_0\hat{\mathbf{z}} \rightarrow \mathbf{q}'_0 = q_0 \cos\theta\hat{\mathbf{z}} + q_0 \sin\theta\hat{\mathbf{x}}, \quad (34)$$

which corresponds to the phonon displacement

$$u_0(\mathbf{x}) = z(\cos\theta - 1) + x \sin\theta. \quad (35)$$

Using $u_0(\mathbf{x})$ inside (33), straightforward analysis then shows that the nonlinear strain u_{zz} and thereby the energy (33) indeed vanish under such rotation, i.e., $\mathcal{H}_{\text{sm}}[u_0] = 0$.

More generally, the global rotation of the smectic state (34) is equivalent to the following transformation of u :

$$u(\mathbf{x}) \rightarrow u(\mathbf{x}) + u_0(\mathbf{x}), \quad (36)$$

as can be seen from its identification with the corresponding phase transformation of $\psi(\mathbf{x})$ in Eq. (26). The latter transforms the nonlinear strain tensor

$$\begin{aligned} u_{zz} &= \partial_z u + \frac{1}{2}(\nabla u)^2 \\ &\rightarrow \partial_z u + \cos\theta - 1 + \frac{1}{2}[\nabla u + (\cos\theta - 1)\hat{\mathbf{z}} + \sin\theta\hat{\mathbf{x}}]^2 \\ &= (\cos\theta\hat{\mathbf{z}} + \sin\theta\hat{\mathbf{x}}) \cdot \nabla u + \frac{1}{2}(\nabla u)^2, \end{aligned} \quad (37)$$

and thereby leaves the form of Hamiltonian (33) unchanged with $\hat{\mathbf{q}} = \hat{\mathbf{z}}$ rotated to $\hat{\mathbf{q}}' = \cos\theta\hat{\mathbf{z}} + \sin\theta\hat{\mathbf{x}}$, i.e., $\mathcal{H}_{\text{sm}}[u(\mathbf{x}) + u_0(\mathbf{x})] = \mathcal{H}_{\text{sm}}[u(\mathbf{x})]$.

B. $N = 2$: XY smectic and FFLO/PDW superfluid

For $N = 2$, in its ordered regime the Hamiltonian (9) encodes a soft planar spin-density wave of XY spins. Physically, this is relevant for frustrated magnetic systems with an easy plane anisotropy and ‘‘striped’’ [e.g., pair-density

wave (PDW), FFLO, and other] nonzero-momentum superfluids [30]. The latter is characterized by a complex field, whose real and imaginary parts are isomorphic to a two-component real vector field. The $U(1)$ symmetry of the superfluid then maps to the $SO(2)$ spin-rotational symmetry of the $N = 2$ spin-smectic. Below, we show that the putative FF (time-reversal-breaking, amplitude uniform) and LO (time-reversal-preserving, amplitude modulated) PDWs states are isomorphic to the coplanar and collinear spin-density waves, emerging from the $N = 2$ field theory, respectively.

The low-energy properties of a striped superfluid can be qualitatively captured by the following order parameter:

$$\Delta_{\text{FFLO}}(\mathbf{x}) = \Delta_+(\mathbf{x})e^{i\mathbf{q}\cdot\mathbf{x}} + \Delta_-(\mathbf{x})e^{-i\mathbf{q}\cdot\mathbf{x}}, \quad (38)$$

where the two complex scalar fields

$$\Delta_{\pm}(\mathbf{x}) = \Delta_{\pm}^0(\mathbf{x})e^{i\phi_{\pm}(\mathbf{x})}, \quad (39)$$

distinguishing between the coplanar and collinear (i.e., the so-called FF and LO) states. The imaginary and real parts of the two complex order parameters in (38) can equivalently be encoded in a spin language, via two real two-component vectors \vec{n}, \vec{m} via

$$\vec{S}_{\text{FFLO}} = \vec{n}(\mathbf{x}) \cos(\mathbf{q} \cdot \mathbf{x}) - \vec{m}(\mathbf{x}) \sin(\mathbf{q} \cdot \mathbf{x}), \quad (40)$$

where

$$\begin{aligned} \vec{n} &= (\Delta_+^R + \Delta_-^R, \Delta_+^I + \Delta_-^I), \\ \vec{m} &= (\Delta_+^I - \Delta_-^I, \Delta_-^R - \Delta_+^R), \end{aligned} \quad (41)$$

with the superscripts R and I , respectively, denoting the real and imaginary parts of the corresponding complex fields.

As in the analysis of the previous subsection, here too the two phases are controlled by the sign of v_2 . For $v_2 < 0$, the Landau free energy (12) selects the collinear state that satisfies the conditions (18) that together with (41) gives $|\Delta_+| = |\Delta_-| \equiv \Delta_0$. The order parameter (38) then reduces to the familiar LO state

$$\Delta_{\text{LO}} = 2\Delta_0 e^{i\phi} \cos(\mathbf{q} \cdot \mathbf{x} + \theta), \quad (42)$$

where the phases

$$\phi = (\phi_+ + \phi_-)/2, \quad \theta = (\phi_+ - \phi_-)/2, \quad (43)$$

are the LO superfluid phase and its smectic phonon, respectively. In terms of the two-component vector order parameters (40), this corresponds to the collinear case with

$$\begin{aligned} \vec{n}_{\text{LO}} &= 2\Delta_0 \cos\theta (\cos\phi, \sin\phi), \\ \vec{m}_{\text{LO}} &= 2\Delta_0 \sin\theta (\cos\phi, \sin\phi). \end{aligned} \quad (44)$$

As detailed below and in Ref. [30], after choosing the minimum $q = q_0$ and dropping constants, the $O(N = 2)_{\text{collinear}}$ σ -model (4) reduces to the Goldstone mode Hamiltonian given by the coupled smectic and XY sectors [29,30],

$$\mathcal{H}_{\text{LO}} = Bu_{qq}^2 + K(\nabla^2 u)^2 + \rho_s^\parallel (\partial_\parallel \phi)^2 + \rho_s^\perp (\partial_\perp \phi)^2, \quad (45)$$

where $u = \theta/q_0$. Notice that ρ_s^\perp vanishes when the current-current interaction $\lambda_2 \rightarrow 0$ (see below and Ref. [30]). Namely, it is required to capture the universal low-energy Goldstone-mode energetics of the LO state.

For $v_2 > 0$, the Landau free energy (12) is minimized by the coplanar state that satisfies the conditions (22), that together with (41) gives $\Delta_+^R \Delta_+^I - \Delta_-^R \Delta_+^I = 0$ and $\Delta_+^R \Delta_-^R + \Delta_+^I \Delta_-^I = 0$, which is equivalent to $\Delta_+ = 0$ or $\Delta_- = 0$. Thus, the order parameter (38) reduces to the FF state

$$\Delta_{\text{FF}} = \Delta_0 e^{i\mathbf{q} \cdot \mathbf{x} + i\phi}, \quad (46)$$

where $\phi = \phi_+$ and the amplitude $\Delta_0 = \Delta_+^0$ is uniform. In terms of the vector order parameter (40), this corresponds to the coplanar state, with orthogonal vectors

$$\vec{n}_{\text{FF}} = \Delta_0(\cos \phi, \sin \phi), \quad \vec{m}_{\text{FF}} = \Delta_0(\sin \phi, -\cos \phi). \quad (47)$$

Thus, the Goldstone-mode $O(N = 2)_{\text{coplanar}}$ σ -model is described by a single smectic phonon (see below and Ref. [30])

$$\mathcal{H}_{\text{FF}} = Bu_{\text{q}}^2 + K(\nabla^2 u)^2, \quad (48)$$

where $u = \phi/q_0$.

We next turn to the discussions of the $N > 2$ coplanar $O(d)$ -symmetric density-wave, which leads to a new class of soft nonlinear $O(N > 2)$ σ -model.

C. $O(N)$ coplanar smectic

For the coplanar helical state, which satisfies the condition (22) and $N \geq 2$, the order parameter can be written as

$$\vec{S} = S_0 \text{Re}[\hat{\psi} e^{i\mathbf{q} \cdot \mathbf{x}}], \quad (49)$$

where

$$\hat{\psi}(\mathbf{x}) = \frac{\hat{n}(\mathbf{x}) + i\hat{m}(\mathbf{x})}{\sqrt{2}} \quad (50)$$

is a complex N -component vector field with $|\hat{\psi}|^2 = 1$, described by orthonormal real vectors, \hat{n} and \hat{m} .

To count the number of Goldstone modes, we first note that the $O(N)$ group consists of $N(N - 1)/2$ generators of rotation that correspond to independent planes in the N -dimensional spin space. For an ordered state that breaks the entire $O(N)$ group, there will be $N(N - 1)/2$ Goldstone modes. For the coplanar state, the symmetry group of the order parameter is $O(N - 2)$ (due to the subtraction of \hat{n} and \hat{m} axes). The Goldstone modes then live on $O(N)/O(N - 2) = S_{N-1} \times S_{N-2}$ manifold with $2N - 3$ Goldstone modes [49].

To derive the Goldstone-mode classical Hamiltonian of the coplanar state, we substitute (49) into (9) and first consider the simplest case with $\lambda_2 = \lambda_3 = 0$, which gives (see details in Appendix A)

$$\mathcal{H}_J = a(q^2 - \bar{q}_0^2)|\nabla \hat{\psi} + i\mathbf{q}\hat{\psi}|^2 + \bar{J}|\nabla^2 \hat{\psi} + 2iq\partial_{\parallel} \hat{\psi}|^2, \quad (51)$$

where the zeroth-order parameters above are given by

$$2a = 4\bar{J} = JS_0^2. \quad (52)$$

By selecting $|\mathbf{q}| \equiv q_0 = \bar{q}_0$ to eliminate the a (first) term in the Hamiltonian above, and expressing the result in terms of the orthonormal triad, we obtain

$$\mathcal{H} = \frac{\bar{J}}{2}(\nabla^2 \hat{n} - 2q_0 \partial_{\parallel} \hat{m})^2 + \frac{\bar{J}}{2}(\nabla^2 \hat{m} + 2q_0 \partial_{\parallel} \hat{n})^2. \quad (53)$$

We stress that this nonlinear $O(N)$ σ -model is fully rotationally invariant for an arbitrary large spin-smectic-layer rotation R , corresponding to $\mathbf{q}_0 \rightarrow \mathbf{q}'_0 = R \cdot \mathbf{q}_0$, where in 3D $\mathbf{q}'_0 =$

$q_0(\cos \theta \hat{\mathbf{z}} + \sin \theta \hat{\mathbf{x}})$ with $\hat{\mathbf{x}}$ any of the axes transverse to $\hat{\mathbf{q}} = \hat{\mathbf{z}}$. With the definition of the order parameter (49), this rotation can be interpreted as the following transformation of \hat{n} and \hat{m} :

$$\begin{aligned} \hat{n} &\rightarrow \hat{n} \cos \chi_R(\mathbf{x}) - \hat{m} \sin \chi_R(\mathbf{x}), \\ \hat{m} &\rightarrow \hat{n} \sin \chi_R(\mathbf{x}) + \hat{m} \cos \chi_R(\mathbf{x}), \end{aligned} \quad (54)$$

where $\chi_R(x, z) = q_0(\cos \theta - 1)z + q_0 \sin \theta x$. Thus, in the helical state the global $spatial O(d)$ rotational symmetry of \mathcal{H} (9) maps onto an *inhomogeneous spin* rotational symmetry $O(\hat{n}, \hat{m})$. It can be straightforwardly verified that the transformation (54) leaves the form of the Hamiltonian (53) unchanged with the \parallel axis rotated to $\hat{\mathbf{q}}' = \cos \theta \hat{\mathbf{z}} + \sin \theta \hat{\mathbf{x}}$.

I. $N = 2$

To further analyze the Hamiltonian (53), we first consider the case of $N = 2$ and parametrize the orthonormal diad as

$$\hat{n}_{N=2} = (\cos \chi, \sin \chi), \quad \hat{m}_{N=2} = (-\sin \chi, \cos \chi), \quad (55)$$

corresponding to

$$\hat{\psi}_{N=2} = \frac{1}{\sqrt{2}} e^{-i\chi} (1, i), \quad (56)$$

where the angle χ is related to the phonon mode along \mathbf{q}_0 by $u = -\chi/q_0$. The Hamiltonian (53) then describes a smectic phonon and reduces to (48) at low energies, where the perpendicular stiffness of $(\nabla_{\perp} u)^2$ vanishes, consistent with our discussion of FF superfluid. As we will see, for a general N , the soft smectic elasticity, enforced by the underlying spatial $O(d)$ rotational symmetry, manifests as a vanishing perpendicular stiffness, $(\hat{m} \cdot \nabla_{\perp} \hat{n})^2$, corresponding to *inhomogeneous* spin rotations in the \hat{n} - \hat{m} plane.

2. $N = 3$

Now we consider $N = 3$ coplanar spin state. The spin space is now spanned by the orthonormal triad $\hat{n}, \hat{m}, \hat{\ell}$, where

$$\hat{\ell}_{\gamma} = \epsilon_{\alpha\beta\gamma} \hat{n}_{\alpha} \hat{m}_{\beta} = \frac{1}{2} \epsilon_{\alpha\beta\gamma} \hat{L}_{\alpha\beta}, \quad (57)$$

with

$$\hat{L}_{\alpha\beta} = \hat{n}_{\alpha} \hat{m}_{\beta} - \hat{m}_{\alpha} \hat{n}_{\beta}. \quad (58)$$

Notably, the $O(3)$ coplanar smectic σ -model can be expressed in terms of the following ‘‘spin connections’’:

$$\mathbf{A} = \hat{m} \cdot \nabla \hat{n} = i\hat{\psi}^* \cdot \nabla \hat{\psi}, \quad \mathbf{D} = \hat{\ell} \cdot \nabla \hat{\psi}, \quad (59)$$

where \mathbf{A} and \mathbf{D} are real and complex spatial vector fields, respectively. To this end, we first note that an arbitrary vector in spin space, \vec{v} , can be expanded in terms of the orthonormal triad,

$$\begin{aligned} \vec{v} &= (\hat{n} \cdot \vec{v})\hat{n} + (\hat{m} \cdot \vec{v})\hat{m} + (\hat{\ell} \cdot \vec{v})\hat{\ell}, \\ &= (\hat{\psi} \cdot \vec{v})\hat{\psi}^* + (\hat{\psi}^* \cdot \vec{v})\hat{\psi} + (\hat{\ell} \cdot \vec{v})\hat{\ell}. \end{aligned} \quad (60)$$

This enables us to express the linear gradient term in (53) as

$$\begin{aligned} (\partial_{\parallel} \hat{m})^2 + (\partial_{\parallel} \hat{n})^2 &= 2(\hat{\mathbf{q}} \cdot \mathbf{A})^2 + 2|\hat{\mathbf{q}} \cdot \mathbf{D}|^2, \\ &= 2(\hat{m} \cdot \partial_{\parallel} \hat{n})^2 + (\partial_{\parallel} \hat{\ell})^2, \end{aligned} \quad (61)$$

where we used

$$|\hat{\mathbf{q}} \cdot \mathbf{D}|^2 = |\hat{\ell} \cdot \partial_{\parallel} \hat{\psi}|^2 = |\hat{\psi} \cdot \partial_{\parallel} \hat{\ell}|^2 = \frac{1}{2}(\partial_{\parallel} \hat{\ell})^2. \quad (62)$$

In the above, the \mathbf{A} (first) and \mathbf{D} (second) terms correspond to the elastic moduli for the along- \mathbf{q}_0 distortions of in-plane (one) and out-of-plane (two) polarizations, respectively. An important feature of the Goldstone-mode σ -model (53) is a vanishing of its transverse stiffness, $A_{\perp}^2 = (\hat{m} \cdot \nabla_{\perp} \hat{n})^2$, guaranteed by the underlying $O(d)$ rotational symmetry of (9), corresponding to rotation of \mathbf{q} . The latter demands a vanishing of the curvature in the transverse component to \mathbf{q}_0 in the thermodynamic potential. The vanished stiffness then follows from the equivalence of the *infinitesimal* shift $\mathbf{q} \rightarrow \mathbf{q} + \delta\mathbf{q}_{\perp}$ and the following transformation:

$$\mathbf{A} \rightarrow \mathbf{A} - \delta\mathbf{q}_{\perp} + O(\delta q_{\perp}^2). \quad (63)$$

In contrast, the vanishing of the transverse stiffness for the out-of-plane polarization $\hat{\ell}$, i.e., a modulus for $|\mathbf{D}_{\perp}|^2 \sim (\nabla_{\perp} \hat{\ell})^2$ in (53), is nonuniversal, unconstrained by any symmetry, and is accidental due to a nongeneric (fine-tuned) nature of (9) for vanishing $\lambda_{2,3}$.

We next derive and analyze a generic coplanar $O(3)$ smectic σ -model by including nonzero λ_2, λ_3 . In particular, we show that λ_3 introduces a nonzero stiffness for $(\nabla_{\perp} \hat{\ell})^2$, controlling the out-of- \hat{n} - \hat{m} -plane fluctuations, leading to our universal Goldstone-mode σ -model of the helical state. This stiffness is also necessary to stabilize model (53), which is otherwise unstable against thermal fluctuations in any dimension (see Sec. III). A complementary view on the importance of the λ_3 coupling and the presence of $(\partial_{\perp} \hat{\ell})^2$ in the Goldstone mode theory is given in Appendix C.

To this end, we examine the contribution of nonzero λ_3 in \mathcal{H} (9) to the σ -model in the coplanar helical state. Relegating the details to Appendixes A and B, using the helical order parameter (49), dropping the oscillatory and constant contributions, we find

$$\begin{aligned} (\partial_i \vec{\mathcal{S}} \cdot \partial_j \vec{\mathcal{S}})^2 &= \frac{S_0^4}{4} \text{Re}[(\partial_i - iq_i) \hat{\psi}^* \cdot (\partial_j + iq_j) \hat{\psi}]^2 \\ &+ \frac{S_0^4}{8} |\partial_i \hat{\psi} \cdot \partial_j \hat{\psi}|^2 \\ &= \frac{S_0^4}{4} \text{Re}[D_i^* D_j + A_i A_j - q_i A_j - q_j A_i + q_i q_j]^2 \\ &+ \frac{S_0^4}{8} |D_i D_j|^2 \\ &\approx \frac{S_0^4}{4} [2|\mathbf{q} \cdot \mathbf{D}|^2 + 4(\mathbf{q} \cdot \mathbf{A})^2 + 2q^2 A^2 \\ &- 4q^2 (\mathbf{q} \cdot \mathbf{A}) + q^4], \end{aligned} \quad (64)$$

where in the last line we only kept terms up to quadratic order in \mathbf{A} and \mathbf{D} . At the minimum of the thermodynamic potential, we remove the linear in \mathbf{A} term with the rotationally invariant strain tensor

$$|\nabla \hat{\psi} + i\mathbf{q} \hat{\psi}|^2 = |\mathbf{D}|^2 + (\mathbf{A} - \mathbf{q})^2, \quad (65)$$

which ensures the stability of the coplanar smectic state. This then leads to the correction

$$S_0^4 [|\mathbf{q} \cdot \mathbf{D}|^2 - q^2 |\mathbf{D}|^2 + 4(\mathbf{q} \cdot \mathbf{A})^2], \quad (66)$$

with the sought-after stabilizing stiffness

$$\begin{aligned} |\mathbf{D}_{\perp}|^2 &= |\mathbf{D}|^2 - |\hat{\mathbf{q}} \cdot \mathbf{D}|^2, \\ &= \frac{1}{2} (\nabla_{\perp} \hat{\ell})^2. \end{aligned} \quad (67)$$

Thus, by including the crucially stabilizing λ_3 contribution to (53), we now have obtained the generic form of the $O(3)$ smectic σ -model of the helical state, as advertised in the Results subsection of the Introduction, Sec. IC,

$$\mathcal{H} = \bar{J} |\nabla^2 \hat{\psi} + 2iq_{\parallel} \partial_{\parallel} \hat{\psi}|^2 + \kappa_{\parallel} (\partial_{\parallel} \hat{\ell})^2 + \kappa_{\perp} (\nabla_{\perp} \hat{\ell})^2, \quad (68)$$

where we included the κ_{\parallel} stiffness, that, as we have seen above, is already contained in the \bar{J} contribution in (61) and can also be generated by other higher-order (in S_0) terms. Neglecting higher-derivative contributions in \bar{J} of (68), an equivalent, smectic form of the $O(3)$ σ -model, expressed in terms of the ‘‘gauge’’ fields, is given by

$$\begin{aligned} \mathcal{H} &= B(q_0 \hat{\mathbf{A}}_{\parallel} - \frac{1}{2} \hat{\mathbf{A}}^2)^2 + K(\nabla \cdot \hat{\mathbf{A}})^2 \\ &+ \kappa_{\parallel} (\partial_{\parallel} \hat{\ell})^2 + \kappa_{\perp} (\nabla_{\perp} \hat{\ell})^2, \end{aligned} \quad (69)$$

where the dimensionless field (not unit vector, $\hat{\mathbf{A}}^2 \neq 1$)

$$\begin{aligned} \hat{\mathbf{A}} &\equiv \mathbf{A}/q_0 = \hat{m} \cdot \nabla \hat{n}/q_0 \\ &\approx \nabla u, \end{aligned} \quad (70)$$

leads to a conventional smectic form (33) for small-angle fluctuations. In the above, the leading contributions to the zeroth-order parameters are

$$K, \kappa_{\parallel} \sim JS_0^2 q_0^2, \quad B \sim JS_0^2 q_0^4, \quad \kappa_{\perp} \sim -\lambda_3 S_0^4 q_0^2, \quad (71)$$

constrained to be $\kappa_{\perp} > 0$ ($\lambda_3 < 0$) for stability of the coplanar helical state.

We close this helical state derivation by noting that the λ_2 term in (9) gives a contribution proportional to

$$(\vec{\mathcal{S}} \times \nabla \vec{\mathcal{S}})^2 = S_0^2 (\nabla \vec{\mathcal{S}})^2, \quad (72)$$

where we used $(\vec{\mathcal{S}} \cdot \nabla \vec{\mathcal{S}})^2 = 0$ and $S^2 = S_0^2$. Since it is proportional to an already present $(\nabla \vec{\mathcal{S}})^2$ term in (9), it simply shifts the minimum q_0 while leaving the form of the resulting Goldstone mode theory (53) unchanged.

Finally, we observe that, in contrast to the stabilizing tensor quartic operator in (64), a scalar quartic term, $(\nabla \vec{\mathcal{S}})^4$, does not introduce any new physics into the $O(3)$ helical σ -model, (68),(69). To see this, observe that in the helical state,

$$\begin{aligned} (\nabla \vec{\mathcal{S}})^4 &= \frac{S_0^4}{4} |\nabla \hat{\psi} + i\mathbf{q} \hat{\psi}|^4 + \frac{S_0^4}{8} |\nabla \hat{\psi} \cdot \nabla \hat{\psi}|^2 \\ &\approx \frac{S_0^4 q^2}{4} [2|\nabla \hat{\psi} + i\mathbf{q} \hat{\psi}|^2 + 4|\hat{\psi}^* \cdot \partial_{\parallel} \hat{\psi}|^2 - q^2], \end{aligned} \quad (73)$$

where in the second line we only kept the terms up to quadratic order in ∇ . Thus, this contribution simply shifts the condition on q that eliminates the first term in (51), only leaving the following correction to the smectic phonon elasticity:

$$|\hat{\psi}^* \cdot \partial_{\parallel} \hat{\psi}|^2 = (\hat{m} \cdot \partial_{\parallel} \hat{n})^2. \quad (74)$$

Thus, the only consequence of this scalar quartic contribution (73) is to modify above zeroth-order (nongeneric) expressions for q , B , and K , and in particular it shows that the elastic constants B and K are independent.

3. $N > 3$

For $N > 3$, the spin space is spanned by N orthonormal vectors \hat{n} , \hat{m} , and $\{\hat{\ell}^\alpha\}$ ($\alpha = 1, \dots, N - 2$). The (quadratic in \mathbf{A} and \mathbf{D}) correction by the λ_3 term, which for $N = 3$ is given by (66), becomes

$$S_0^4[|\mathbf{q} \cdot \mathbf{D}^\alpha|^2 - q^2|\mathbf{D}^\alpha|^2 + 4(\mathbf{q} \cdot \mathbf{A})^2], \quad (75)$$

where $\mathbf{D}^\alpha = \hat{\ell}^\alpha \cdot \nabla \hat{\psi}$. It now gives the following stabilizing out-of-plane contribution to the $O(N > 3)$ σ -model,

$$\begin{aligned} |\mathbf{D}_\perp^\alpha|^2 &= |\hat{\ell}^\alpha \cdot \nabla_\perp \hat{\psi}|^2 = |\nabla_\perp \hat{\psi}|^2 - (i\hat{\psi}^* \cdot \nabla_\perp \hat{\psi})^2 \\ &= \frac{1}{4}(\nabla_\perp \hat{L})^2, \end{aligned} \quad (76)$$

where in the last line we expressed it in terms of \hat{L} , the components of out-of-plane fluctuations defined in (58), using the identity

$$\begin{aligned} \frac{1}{2}(\nabla \hat{L}_{\alpha\beta})^2 &= \nabla(\hat{n}_\alpha \hat{m}_\beta) \nabla(\hat{n}_\alpha \hat{m}_\beta) - \nabla(\hat{n}_\alpha \hat{m}_\beta) \nabla(\hat{n}_\beta \hat{m}_\alpha) \\ &= (\nabla \hat{n})^2 + (\nabla \hat{m})^2 - 2(\hat{m} \cdot \nabla \hat{n})^2 \\ &= 2|\nabla \hat{\psi}|^2 - 2(i\hat{\psi}^* \cdot \nabla \hat{\psi})^2. \end{aligned} \quad (77)$$

Thus, as advertised in the Results subsection of the Introduction, Sec. IC, the $O(N)$ smectic σ -model is given by

$$\mathcal{H} = \bar{J}|\nabla^2 \hat{\psi} + 2iq\partial_\parallel \hat{\psi}|^2 + \kappa_\parallel(\partial_\parallel \hat{L})^2 + \kappa_\perp(\nabla_\perp \hat{L})^2. \quad (78)$$

When higher-order gradients are neglected, it reduces to a form resembling a conventional smectic,

$$\begin{aligned} \mathcal{H} &= B(q_0 \hat{\mathbf{A}}_\parallel - \frac{1}{2} \hat{\mathbf{A}}^2)^2 + K(\nabla \cdot \hat{\mathbf{A}})^2 \\ &\quad + \kappa_\parallel(\partial_\parallel \hat{L})^2 + \kappa_\perp(\nabla_\perp \hat{L})^2. \end{aligned} \quad (79)$$

D. $O(N)$ collinear smectic

We next derive the Goldstone-mode smectic σ -model for the collinear state for a general N . As discussed in Sec. II, the order parameter of the collinear state can be parametrized as

$$\vec{S} = S_0 \text{Re}[\hat{\psi}(\mathbf{x})e^{iq \cdot \mathbf{x}}], \quad (80)$$

with

$$\hat{\psi}(\mathbf{x}) = \hat{n}(\mathbf{x})e^{iqu(\mathbf{x})}, \quad (81)$$

described by a unit ‘‘polarization’’ vector, $\hat{n}(\mathbf{x})$, and a phonon mode, $u(\mathbf{x})$, with a parametrization redundancy that requires identification of \hat{n} with $-\hat{n}$, which is already accounted for by $qu = \pi$. There are thus N Goldstone modes living on the $S_{N-1} \times S_1/Z_2$ compact manifold. We also note that (in contrast to the coplanar state) the magnitude of such a linearly polarized spin-density-wave state oscillates in space, and thus (81) corresponds to a *coarse-grained* spin-density order parameter.

We can now derive the $O(N)$ collinear smectic σ -model using the representation (80) inside the J piece of \mathcal{H} in (9). Relegating technical details to Appendix A, we obtain

$$\begin{aligned} \mathcal{H}_J &= a(q^2 - \bar{q}_0^2)[u_{qq} + (\nabla \hat{n})^2/2q^2] + Bu_{qq}^2 + K(\nabla^2 u)^2 \\ &\quad + \kappa_\parallel(\partial_\parallel \hat{n} + \nabla u \cdot \nabla \hat{n})^2 + \alpha(\nabla^2 \hat{n})^2 + c(\nabla \hat{n})^2 u_{qq}, \end{aligned} \quad (82)$$

where $\partial_\parallel \equiv \partial_q = \hat{\mathbf{q}} \cdot \nabla$, the familiar nonlinear smectic strain u_{qq} is given by (30), and the zeroth-order elastic moduli are

$$\alpha = \frac{JS_0^2}{4}, \quad a = 4K = \kappa_\parallel = c = JS_0^2 q^2, \quad B = JS_0^2 q^4. \quad (83)$$

We note that, as expected on general $O(d)$ symmetry grounds, at the energy minimum $|\mathbf{q}| \equiv q_0 = \bar{q}_0$, the phonon mode is ‘‘soft’’ (i.e., controlled by higher derivative elasticity), with a vanishing transverse-to- \mathbf{q} stiffness, $(\nabla_\perp u)^2$. This is enforced by the underlying $O(d)$ rotational invariance of \mathcal{H} in (9) (including fluctuations), which corresponds to an arbitrary rotation of the spontaneously chosen \mathbf{q} . This then ensures the vanishing of the transverse-to- \mathbf{q} curvature in the thermodynamics potential at the minimum \mathbf{q}_0 , with the zero stiffness that then follows from the equivalence of the following transformations:

$$\mathbf{q} \rightarrow \mathbf{q} + \delta \mathbf{q}_\perp \Leftrightarrow qu \rightarrow qu + \delta \mathbf{q}_\perp \cdot \mathbf{x}, \quad (84)$$

where $\mathbf{q} \cdot \delta \mathbf{q}_\perp = 0$, coming from the definition of the order parameter in (80).

In contrast, the vanishing of the transverse stiffness of the Goldstone mode $(\nabla_\perp \hat{n})^2$ is a purely accidental property of the J term in (9), and is generically expected to be nonzero for the full \mathcal{H} . Indeed, by including the λ_2 term (with details given in Appendix A), we find

$$\begin{aligned} (\vec{S} \times \nabla \vec{S})^2 &= S^2(\nabla \vec{S})^2 - (\vec{S} \cdot \nabla \vec{S})^2 \\ &= \frac{3S_0^4}{8}(\nabla \hat{n})^2, \end{aligned} \quad (85)$$

which gives a nonzero transverse κ_\perp stiffness for \hat{n} gradient deformations. With this, and choosing $\mathbf{q} = q_0 \hat{\mathbf{z}}$, we finally obtain the $O(N)$ collinear smectic σ -model for its N Goldstone modes,

$$\begin{aligned} \mathcal{H} &= Bu_{zz}^2 + K(\nabla^2 u)^2 + c(\nabla \hat{n})^2 u_{zz} \\ &\quad + \kappa_\parallel(\partial_z \hat{n} + \nabla u \cdot \nabla \hat{n})^2 + \kappa_\perp(\nabla_\perp \hat{n})^2, \end{aligned} \quad (86)$$

where the zeroth-order stiffnesses are given by

$$K, \kappa_\parallel \sim JS_0^2 q_0^2, \quad B \sim JS_0^4 q_0^4, \quad \kappa_\perp \sim \lambda_2 S_0^4. \quad (87)$$

Neglecting symmetry-allowed nonlinearities in u and \hat{n} ,

$$(\nabla \hat{n})^2 u_{zz}, \quad (\nabla u \cdot \nabla \hat{n}) \partial_z \hat{n}, \quad (\nabla u \cdot \nabla \hat{n})^2, \quad (88)$$

leads to two decoupled sectors of a conventional scalar smectic in u and the standard $O(N)$ σ -model in \hat{n} (4). We leave the open question of the effects of these couplings to a future study. Other terms like λ_3 also give a corrections to κ_\perp (proportional to $JS_0^4 q_0^2$), but they do not change the universal long-wavelength form (86). As expected, for $N = 2$, the Hamiltonian density (86) reduces to the smectic σ -model of the LO superfluid, (45), with the superfluid phase representing the single Euler angle of \hat{n} , corresponding to the complex superfluid order parameter.

III. THERMAL FLUCTUATIONS IN THE $O(N = 3)$ SMECTIC STATES

Having established the corresponding smectic coplanar and collinear σ -models, we next analyze the thermodynamic

properties of these smectic spin-density wave states, with a focus on the physical case of $N = 3$. We limit our analysis to classical statistical mechanics at the Gaussian fixed point, with the Goldstone-modes partition function given by

$$Z = \int \mathcal{D}\hat{\psi} \mathcal{D}\hat{\psi}^* e^{-\beta \int d^d x \mathcal{H}[\hat{\psi}, \hat{\psi}^*]}, \quad (89)$$

where $\beta = T^{-1}$ ($k_B = 1$ throughout) and $\hat{\psi}$ given by (50) and (81) for the coplanar and collinear states, respectively.

Namely, below we introduce the angular fields representation of the Goldstone modes in the Hamiltonian density $\mathcal{H}[\hat{\psi}, \hat{\psi}^*]$ for these two $O(3)$ smectic states. Then, we examine their stability to small thermal fluctuations within a Gaussian approximation, followed by a discussion of possible consequences of the nonlinearities and symmetry-breaking perturbations. We will then calculate Goldstone modes' correlation functions that control low-energy, long-wavelength scattering and thermodynamics.

A. Angular representation of Goldstone modes

1. Collinear state

As discussed in the previous sections, the $N = 3$ collinear smectic state (80) is characterized by a smectic phonon u and a unit spin vector \hat{n} . The latter can be parametrized by

$$\hat{n}(\mathbf{x}) = \cos \theta \cos \phi \hat{e}_1 + \cos \theta \sin \phi \hat{e}_2 + \sin \theta \hat{e}_3, \quad (90)$$

where we chose an orthonormal frame $\hat{e}_1, \hat{e}_2, \hat{e}_3 = \hat{e}_1 \times \hat{e}_2$, such that for small fluctuation of these angular Goldstone modes, $\theta(\mathbf{x})$ and $\phi(\mathbf{x})$,

$$\hat{n}(\mathbf{x}) \approx \hat{e}_1 + \phi \hat{e}_2 + \theta \hat{e}_3. \quad (91)$$

Neglecting higher-order gradients, the Hamiltonian density (86) is then given by

$$\begin{aligned} \mathcal{H} = & Bu_{qq}^2 + K(\nabla^2 u)^2 + \kappa_{\parallel}(\partial_{\parallel} \theta)^2 + \kappa_{\parallel} \cos^2 \theta (\partial_{\parallel} \phi)^2 \\ & + \kappa_{\perp}(\nabla_{\perp} \theta)^2 + \kappa_{\perp} \cos^2 \theta (\nabla_{\perp} \phi)^2. \end{aligned} \quad (92)$$

2. Coplanar state

The fluctuations of the $N = 3$ coplanar state (49) are parametrized by an orthonormal triad, $\hat{n}, \hat{m}, \hat{\ell} = \hat{n} \times \hat{m}$. In terms of the complex vector field $\hat{\psi} = \hat{n} + i\hat{m}$, this can be parametrized by

$$\begin{aligned} \hat{\ell} &= \cos \theta \cos \phi \hat{e}_1 + \cos \theta \sin \phi \hat{e}_2 + \sin \theta \hat{e}_3, \\ \hat{\psi} &= [(\sin \theta \cos \phi - i \sin \phi) \hat{e}_1 + (\sin \theta \sin \phi + i \cos \phi) \hat{e}_2 \\ &\quad - \cos \theta \hat{e}_3] i e^{-i\chi} / \sqrt{2}, \end{aligned} \quad (93)$$

where θ and ϕ are Euler angles that parametrize the orientation of $\hat{\ell}$ and χ the rotation around $\hat{\ell}$. In the small-angle approximation, this gives

$$\begin{aligned} \hat{\ell} &\approx \hat{e}_1 + \phi \hat{e}_2 + \theta \hat{e}_3, \\ \hat{n} &\approx \phi \hat{e}_1 - \hat{e}_2 - \chi \hat{e}_3, \\ \hat{m} &\approx \theta \hat{e}_1 + \chi \hat{e}_2 - \hat{e}_3. \end{aligned} \quad (94)$$

The coplanar Hamiltonian density (69) is then given by the same form of the collinear state Hamiltonian (92), with the

gradient of the smectic phonon replaced by

$$\nabla u \rightarrow \hat{\mathbf{A}} = \frac{1}{q_0} \sin \theta \nabla \phi + \nabla u, \quad (95)$$

where the third Euler angle χ is associated with the smectic phonon by $\chi = q_0 u$. We note that although the coplanar and collinear smectic states are quite different, their low-energy excitations only differ by the nonlinearities in $\hat{\mathbf{A}}$.

3. Harmonic theory of $O(3)$ smectic

As discussed above, the Goldstone mode models for the $N = 3$ collinear and coplanar states arise from the spontaneous periodic ordering of spins at wave vector \mathbf{q}_0 , which leads to an order parameter that breaks the $O(N = 3)$ -spin and $O(d = 3)$ -spatial symmetries. Because the two states only differ from each other by the nonlinearities (95), at the harmonic level the collinear and coplanar states are described by the same low-energy Hamiltonian density,

$$\mathcal{H}_0 = \mathcal{H}_{0,\text{sm}}[u] + \mathcal{H}_{0,\text{spin}}[\theta, \phi], \quad (96)$$

where

$$\begin{aligned} \mathcal{H}_{0,\text{sm}}[u] &= B(\partial_{\parallel} u)^2 + K(\nabla^2 u)^2, \\ \mathcal{H}_{0,\text{spin}}[\theta, \phi] &= \sum_{\varphi=\theta, \phi} [\kappa_{\parallel}(\partial_{\parallel} \varphi)^2 + \kappa_{\perp}(\nabla_{\perp} \varphi)^2], \end{aligned} \quad (97)$$

with the zeroth-order elastic moduli given by (71) and (87) for the coplanar and collinear states, respectively. Thus, the harmonic model (96) consists of decoupled smectic and two XY Goldstone modes.

At higher energies, however, the collinear and coplanar states acquire distinct corrections to (96), which can become particularly important as near the melting transition where the ratio of the XY moduli, $\kappa_{\perp}/\kappa_{\parallel} \sim S_0^2$, vanishes as $S_0 \rightarrow 0$. For the collinear state, the higher-order term, $\alpha(\nabla^2 \hat{n})^2$, in (82) leads to the spin Goldstone mode Hamiltonian

$$\begin{aligned} \mathcal{H}_{0,\text{spin}}^{\text{collinear}}[\theta, \phi] &= \sum_{\varphi=\theta, \phi} [\kappa_{\parallel}(\partial_{\parallel} \varphi)^2 + \kappa_{\perp}(\nabla_{\perp} \varphi)^2] \\ &\quad + \alpha(\nabla^2 \theta)^2 + \alpha(\nabla^2 \phi)^2 \end{aligned} \quad (98)$$

with $\alpha = JS_0^2$. For the coplanar state, the leading correction in (53) instead gives

$$\begin{aligned} \mathcal{H}_{0,\text{spin}}^{\text{coplanar}}[\theta, \phi] &= \bar{J}(\nabla^2 \theta - 2q_0 \partial_{\parallel} \phi)^2 + \bar{J}(\nabla^2 \phi + 2q_0 \partial_{\parallel} \theta)^2 \\ &\quad + \kappa_{\perp}(\nabla_{\perp} \theta)^2 + \kappa_{\perp}(\nabla_{\perp} \phi)^2 \end{aligned} \quad (99)$$

with $\bar{J} = JS_0^2/4$ and $\kappa_{\parallel} = 4\bar{J}q_0^2$.

4. Symmetry-breaking perturbations

Before analyzing thermal fluctuations in these $O(3)$ smectic states, we note that in the solid-state realizations there are two types of natural symmetry-breaking perturbations on the Hamiltonian (9), as we now discuss.

First, in the presence of the underlying lattice that breaks $O(d = 3)$ -spatial rotational symmetry but preserves $O(N = 3)$ -spin symmetry, the ordering wave vector \mathbf{q}_0 will get energetically pinned to high-symmetry crystalline axes, either in a microscopic Hamiltonian by higher-order exchange couplings or via quantum and/or thermal order-by-disorder phenomena

[33,35]. This in turn introduces a transverse (to \mathbf{q}_0) stiffness, B_\perp , to the spin-density pseudophonon mode u in the smectic sector, leading to $\mathcal{H}_{0,\text{sm}} \rightarrow \mathcal{H}_{0,\text{sm}}^{\text{crystal}}$, where

$$\begin{aligned} \mathcal{H}_{0,\text{sm}}^{\text{crystal}} &= B(\partial_\parallel u)^2 + B_\perp(\partial_\perp u)^2 + K(\nabla^2 u)^2, \\ &\approx B(\partial_\parallel u)^2 + B_\perp(\partial_\perp u)^2. \end{aligned} \quad (100)$$

Secondly, the ever-present SOC locks the orientation of spin to \mathbf{q} , breaking the independent $O(N = 3) \times O(d = 3)$ symmetry down to its diagonal subgroup, with the reduced $O(3)$ symmetry further broken by the accompanying crystalline anisotropies. In the case of the coplanar state, this will gap out the spin sector [$\mathcal{H}_{0,\text{spin}}$ in (96)]. For \mathbf{q}_0 that is spatially incommensurate with the lattice, this will then reduce Goldstone modes down to a single conventional XY phonon of a standard discrete spin-density wave.

Nevertheless, in the case of weak symmetry-breaking perturbations, based on a number of experimental realizations [37–41,50–53], we expect an extended range of length scales over which our $O(d) \times O(N)$ description will apply, but we expect it to asymptotically crossover to weakly fluctuating behavior of conventional spin-density waves.

B. Stability

As found in the previous subsection, at a quadratic level the low-energy Hamiltonian densities are identical for the collinear and coplanar spin-smectic states, given by (96), with decoupled Goldstone modes u , θ , and ϕ . We first analyze thermal fluctuations at this harmonic order, and then discuss the effects of nonlinearities.

1. Gaussian fluctuations

The stability of the $O(3)$ smectic states is characterized by their local Goldstone-mode thermal root-mean-squared (rms) fluctuations, $\langle u^2 \rangle$, $\langle \theta^2 \rangle$, $\langle \phi^2 \rangle$. The divergence of these quantities with system size in the thermodynamic limit is a signature of the instability of the spatial (for $\langle u^2 \rangle$) and spin (for $\langle \theta^2 \rangle$ and $\langle \phi^2 \rangle$) orders.

We first analyze the stability of the spatially uniform component of the magnetic order, characterized by (taking $\kappa = \kappa_\parallel = \kappa_\perp$ for simplicity)

$$\begin{aligned} \langle \theta^2 \rangle = \langle \phi^2 \rangle &= \frac{T}{2\kappa} \int_{L^{-1}}^{a^{-1}} \frac{dq^d}{(2\pi)^d} \frac{1}{q^2} \\ &\sim \frac{T}{\kappa} \times \begin{cases} L^{2-d}, & d < 2, \\ \ln(L/a), & d = 2, \\ a^{2-d}, & d > 2, \end{cases} \end{aligned} \quad (101)$$

where L is the system size, a is the UV cutoff length scale, T is the temperature, and we neglected subordinate contributions in $a/L \ll 1$. Thus, the spin orientational order is unstable for $d \leq 2$. This is a manifestation in the uniform spin sector of our system of the Hohenberg-Mermin-Wagner theorems [54,55], where in a classical field theory at nonzero temperature, controlled by a Gaussian fixed point, a continuous symmetry can only be spontaneously broken for $d > 2$. As a side note, for $\kappa_\perp \rightarrow 0$, the coplanar state [with Hamiltonian (99) that includes higher-order terms] exhibits fluctuations

$\langle \theta \rangle^2 = \langle \phi \rangle^2 \sim \int_{\mathbf{q}} (q_z - q^2)^{-2} \sim L$ that diverge with system size. Thus, the coplanar state is unstable in any dimensions without the stabilizing modulus κ_\perp , which, as we discussed above, arose from including a nonzero λ_3 modulus.

The stability of the translational symmetry breaking is characterized by rms fluctuations of the smecticlike phonon, given by

$$\begin{aligned} \langle u^2 \rangle &= \frac{T}{2} \int_{L_\perp^{-1}}^{a_\perp^{-1}} \frac{dq_\parallel dq_\perp^{d-1}}{(2\pi)^d} \frac{1}{Bq_\parallel^2 + Kq_\perp^4} \\ &= \frac{T}{4\sqrt{BK}} \int_{L_\perp^{-1}}^{a_\perp^{-1}} \frac{dq_\perp^{d-1}}{(2\pi)^{d-1}} \frac{1}{q_\perp^2} \\ &\sim \frac{T}{\sqrt{BK}} \times \begin{cases} L_\perp^{3-d}, & d < 3, \\ \ln(L_\perp/a_\perp), & d = 3, \\ a_\perp^{3-d}, & d > 3, \end{cases} \end{aligned} \quad (102)$$

where L_\perp and a_\perp are, respectively, the system size and UV lattice cutoff, transverse to \mathbf{q} , and again we only kept leading contributions in $L_\perp \gg a_\perp$. The lower-critical dimension of the smectic (density-wave) order is thus given by $d_{lc} = 3$, where the system exhibits logarithmically diverging thermal fluctuations [11,56].

Thus, at the Gaussian level, we expect that the $O(3)$ smecticlike helical states will exhibit long-range magnetic and quasi-long-range translational orders in three dimensions. However, as emphasized in Sec. III A 4, in crystalline materials (but not in atomic gases), the presence of lattice anisotropies and SOC introduces stabilizing elastic moduli. These moduli give rise to conventional Goldstone modes at low energies, characterized by $d_{lc} = 2$ and thus leading to long-range order in three dimensions, as in conventional XY and Heisenberg models. However, for weak symmetry-breaking perturbations, we expect strong smecticlike fluctuations in three dimensions extending over long crossover length scales.

2. Nonlinearities

As discussed above, the collinear and coplanar states are both characterized by an $O(N = 3)$ unit vector and a smecticlike phonon, but with different symmetry-allowed nonlinear coupling terms. Below, we will first discuss the two sectors of Goldstone modes that have been studied individually over the past few decades, and then we will comment on the nonlinear couplings between them.

The $O(N)$ σ -model was first studied by Polyakov [6], Nelson, and Pelcovits [7] using a perturbative renormalization group (RG) in $d = 2 + \epsilon$, which shows that for $N > 2$ the ferromagnet-paramagnet (FM-PM) transition is described by a *critical* fixed point at $T_c \sim \epsilon/(N - 2)$, as illustrated in Fig. 4(a). Consequently, the ordered state is unstable in 2D ($T_c = 0$) at any nonzero temperatures, where the correlation length of the order parameter is finite. This is in contrast to the $N = 2$ XY model that has vanished nonlinearity, and at low temperatures exhibits a quasi-long-range-ordered Kosterlitz-Thouless phase.

The smectic Goldstone mode theory was studied by Grinstein and Pelcovits [12,13] using RG for $d = 3$, by

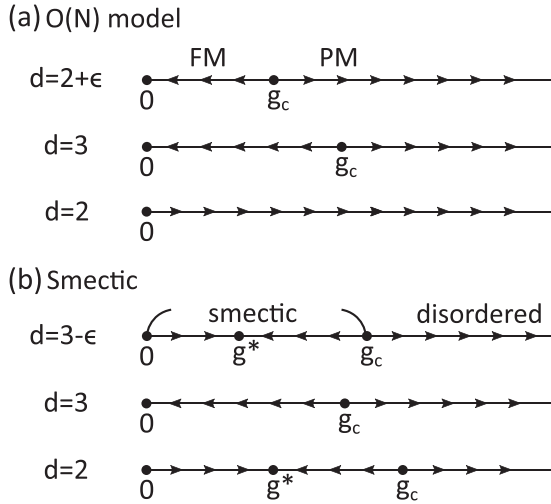


FIG. 4. Schematic renormalization group (RG) flows for a classical (a) ferromagnetic state in the $O(N > 2)$ model and for (b) the smectic state in various dimensions. (a) The dimensionless coupling $g \sim T/\kappa$. The FM-PM phase transition is controlled by the *repulsive* critical point at $g = g_c \sim \epsilon/(N-2)$. For $d > 2$, there is a stable ferromagnetic state at low temperatures, while for $d = 2$, $g_c = 0$, signifying the instability of the classical ferromagnetic state, destroyed by thermal fluctuations. (b) The dimensionless coupling $g \sim T\sqrt{B/K^3}$. At low temperatures $g < g_c$, the smectic state is characterized by a nontrivial infrared *attractive* fixed point at $g = g^* \sim \epsilon$, but it becomes unstable below its lower-critical dimension $d_{lc} = 3$.

Golubović and Wang [57] in $d = 2$, and by Radzihovsky in $d = 3 - \epsilon$ [30]. Remarkably, for $d = 3 - \epsilon$, the smectic ordered state is described by an *attractive* fixed point at $g^* \sim \epsilon$ —a stable critical phase [see Fig. 4(b)] [58]. However, we note that these analyses all consider pure elastic models that neglect topological defects—dislocations in the layered structure, which undoubtedly unbind in 2D at any nonzero temperatures [59]. Thus, these critical phase correlations only extend out to lengths corresponding to distance between topological defects, beyond which the state crosses over to a translationally disordered nematic.

Now we consider the coupling between the two sectors. For the collinear state, the leading-order couplings in (88) in angular representation are given by

$$(\nabla_{\perp} \hat{n})^2 (\partial_{\parallel} u), \quad (\partial_{\parallel} \hat{n}) \cdot (\nabla_{\perp} \hat{n} \cdot \nabla_{\perp} u), \quad (\nabla_{\perp} \hat{n})^2 (\nabla_{\perp} u)^2. \quad (103)$$

At $d = 3$, the only marginal correction to the elastic moduli is $\langle (\nabla_{\perp} u)^2 (\nabla_{\perp} u)^2 \rangle$ and the remaining are irrelevant. Therefore, all coupling terms are irrelevant and at low energies the two sectors are decoupled, described by the RG flows in Fig. 4, all of which are asymptotically identical to those in Refs. [12,13,30]. A similar argument applies to the coplanar state. However, as discussed in Eq. (95), the Goldstone-mode Hamiltonian is distinct from the collinear state by a replacement

$$q_0 \nabla u \rightarrow \sin \theta \nabla \phi + q_0 \nabla u. \quad (104)$$

As a result, smectic phonon u and the spin field $\hat{\ell}$ are intrinsically coupled in the low-energy Hamiltonian (69). This

implies that the spin field $\hat{\ell}$ can acquire a universal power-law correction to its elastic moduli, which are distinct from the \hat{n} in collinear state. We leave the resulting RG analysis to future studies.

C. Two-point correlation function of Goldstone modes

Next we calculate the two-point correlation functions of the Goldstone modes. This not only provides spatially resolved properties of the system but also serves as the first step towards a calculation of the structure factor of the following subsection. We note that as discussed above, in principle all Goldstone modes are coupled. However, because they are subdominant, below we neglect the coupling between the smectic (χ) and magnetic (θ and ϕ) sectors, a valid approximation at low energies.

1. Smectic Goldstone mode

Both the collinear and coplanar states are characterized by a smectic phonon, whose correlation function is given by the following logarithmic Caillé form [56]:

$$\begin{aligned} C_{\text{sm}}(\mathbf{x}) &\equiv \langle [u(\mathbf{x}) - u(0)]^2 \rangle = T \int^{\frac{1}{a}} \frac{dq_{\parallel} dq_{\perp}^2}{(2\pi)^3} \frac{1 - e^{i\mathbf{q}\cdot\mathbf{x}}}{Bq_{\parallel}^2 + Kq_{\perp}^4} \\ &\approx T \int^{\frac{1}{a}} \frac{dq_{\parallel} dq_{\perp}^2}{(2\pi)^3} \frac{1 - e^{i\mathbf{q}\cdot\mathbf{x}}}{Bq_{\parallel}^2 + Kq_{\perp}^4} \\ &= \frac{T}{4\pi\sqrt{BK}} \left[\ln\left(\frac{x_{\perp}}{a}\right) - \frac{1}{2} \text{Ei}\left(\frac{-x_{\perp}^2}{4\lambda|x_{\parallel}|}\right) \right] \\ &\approx \begin{cases} \frac{T}{4\pi\sqrt{BK}} \ln\left(\frac{x_{\perp}}{a}\right), & x_{\perp} \gg \sqrt{\lambda|x_{\parallel}|}, \\ \frac{T}{8\pi\sqrt{BK}} \ln\left(\frac{\lambda|x_{\parallel}|}{a^2}\right), & x_{\perp} \ll \sqrt{\lambda|x_{\parallel}|}, \end{cases} \end{aligned} \quad (105)$$

which exhibits an anisotropic correlation at long scales, with the coefficients in front of the \ln functions differing by a factor 2 in the perpendicular and parallel directions. In the above, $\text{Ei}(x)$ is the exponential-integral function. $\lambda = \sqrt{K/B}$ is the penetration length that characterizes the anisotropy of the smectic state.

In the presence of weak lattice anisotropy, where the spatial rotational symmetry is explicitly broken, the smectic mode is perturbed by a stabilizing modulus, $B_{\perp} \ll B$, with the Hamiltonian given by (100). This deforms the correlation function to be of the following form:

$$C_{\text{sm}}^{\text{crystal}}(\mathbf{x}) = T \int_{\mathbf{q}} \frac{1 - e^{i\mathbf{q}\cdot\mathbf{x}}}{Bq_{\parallel}^2 + B_{\perp}q_{\perp}^2 + Kq_{\perp}^4}. \quad (106)$$

As illustrated in Fig. 5, this introduces a crossover scale $\lambda_{\perp} = \sqrt{K/B_{\perp}}$ in 3D separating the logarithmic ($x_{\parallel} < \lambda_{\perp}^2/\lambda$, $x_{\perp} < \lambda_{\perp}$) and long-range-ordered ($x_{\parallel} > \lambda_{\perp}^2/\lambda$, $x_{\perp} > \lambda_{\perp}$) regimes.

2. Spin Goldstone modes

For the spin sector, the Goldstone modes $\varphi = \theta, \phi$ at low energies are described by the XY model form, with their

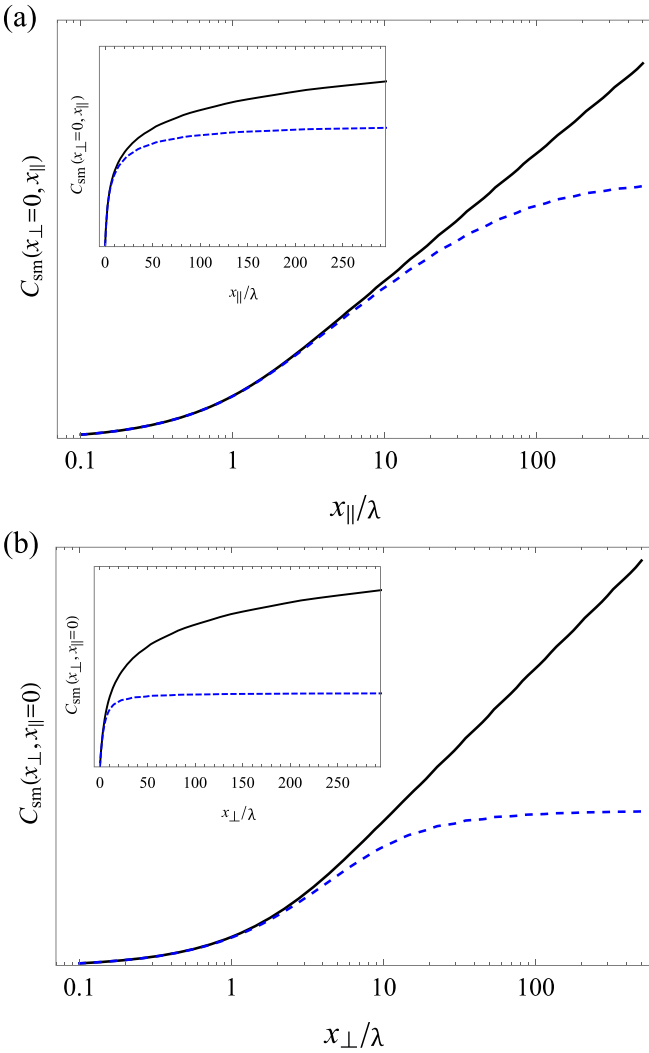


FIG. 5. Linear-log plot of 3D two-point correlation function of a smectic phonon with $\lambda = \sqrt{K/B} = a$ along (a) x_{\parallel} and (b) x_{\perp} . The black-solid and blue-dashed curves correspond to the cases $\lambda_{\perp} = \sqrt{K/B_{\perp}} = \infty$ and 5λ , respectively. The crossover scales from the smectic to XY fluctuations are given by $\lambda_{\perp} = 5\lambda$ and $\lambda_{\parallel}^2/\lambda = 25\lambda$ in the perpendicular and parallel directions, respectively. Inset: same plot in linear scales.

correlation function given by

$$\begin{aligned}
 C_{xy,\varphi}(\mathbf{x}) &= \langle [\varphi(\mathbf{x}) - \varphi(0)]^2 \rangle \\
 &= T \int \frac{dq_{\parallel} dq_{\perp}^2}{(2\pi)^3} \frac{1 - e^{i\mathbf{q}\cdot\mathbf{x}}}{\kappa_{\parallel} q_{\parallel}^2 + \kappa_{\perp} q_{\perp}^2} \\
 &= \frac{T}{2\pi^2 \kappa_{\parallel}^{1/2} \kappa_{\perp}} \int_0^{1/\tilde{x}(a)} dp \left(1 - \frac{\sin(p\tilde{x})}{p\tilde{x}} \right) \\
 &\approx \frac{T}{2\pi^2 \kappa_{\parallel}^{1/2} \kappa_{\perp}} \left(\frac{1}{\tilde{x}(a)} - \frac{1}{\tilde{x}(\mathbf{x})} \right), \quad (107)
 \end{aligned}$$

where

$$\tilde{x}(\mathbf{x}) = \sqrt{\frac{x_{\parallel}^2}{\kappa_{\parallel}} + \frac{x_{\perp}^2}{\kappa_{\perp}}}, \quad \tilde{x}(a) = a\sqrt{\kappa_{\parallel}^{-1} + \kappa_{\perp}^{-1}}. \quad (108)$$

The correlator consists of constant and power-law parts, which, as discussed below, gives rise to two power-law contributions to the peaks of the static structure factor.

As discussed in Sec. III A 4, in the presence of SOC that locks the spins perpendicular to \mathbf{q}_0 , the magnetic Goldstone modes can be pinned with a gap k_p^2 , leading to

$$\begin{aligned}
 C_{xy}^{\text{soc}}(\mathbf{x}) &= T \int \frac{dq_{\parallel} dq_{\perp}^2}{(2\pi)^3} \frac{1 - e^{i\mathbf{q}\cdot\mathbf{x}}}{\kappa_{\parallel} q_{\parallel}^2 + \kappa_{\perp} q_{\perp}^2 + k_p^2} \\
 &= \frac{T}{2\pi^2 \kappa_{\parallel}^{1/2} \kappa_{\perp}} \int_0^{1/\tilde{x}(a)} \frac{dp}{1 + k_p^2/p^2} \left(1 - \frac{\sin(p\tilde{x})}{p\tilde{x}} \right) \\
 &\approx \frac{T}{2\pi^2 \kappa_{\parallel}^{1/2} \kappa_{\perp}} \left(\frac{e^{-k_p \tilde{x}(a)}}{\tilde{x}(a)} - \frac{e^{-k_p \tilde{x}(\mathbf{x})}}{\tilde{x}(\mathbf{x})} \right), \quad (109)
 \end{aligned}$$

where the gap introduces crossover length scales $\xi_{\parallel/\perp}^{\text{soc}} = \sqrt{\kappa_{\parallel/\perp}/k_p}$ for the parallel/perpendicular directions, beyond which the spin fluctuations are suppressed.

D. Structure factor

The static spin structure factor is an important experimental characterization of magnetic ordering. Theoretically, this is proportional to the equal-time spin-spin correlation function,

$$\mathcal{S}(\mathbf{q}) = \frac{1}{V} \int_{\mathbf{x}, \mathbf{x}'} e^{i\mathbf{q}\cdot(\mathbf{x}-\mathbf{x}')} \langle \vec{S}(\mathbf{x}) \cdot \vec{S}(\mathbf{x}') \rangle, \quad (110)$$

where V is the volume of the system. Below, we calculate the structure factor for the soft spin-density waves using the Gaussian theory (96), focusing on its asymptotic long-wavelength behaviors and the effects of symmetry-breaking perturbations that are relevant in real materials. As detailed in Appendix D, at the Gaussian level, the asymptotic behavior of the structure factor for the collinear and coplanar states takes the same form:

$$\begin{aligned}
 \mathcal{S}(\mathbf{q}) &\sim \int_{\mathbf{x}} [e^{i(\mathbf{q}-\mathbf{q}_0)\cdot\mathbf{x}} + e^{i(\mathbf{q}+\mathbf{q}_0)\cdot\mathbf{x}}] \text{Tr} D(\mathbf{x}) e^{-\frac{1}{2} q_0^2 C_{\text{sm}}(\mathbf{x})} \\
 &= P_0(\mathbf{q}) + P(\mathbf{q} - \mathbf{q}_0) + P(\mathbf{q} + \mathbf{q}_0) \quad (111)
 \end{aligned}$$

with

$$P(\mathbf{k}) = P_{\text{sm}}(\mathbf{k}) + P_{xy}(\mathbf{k}), \quad (112)$$

where we retained only the fundamental $\pm\mathbf{q}_0$ quasi-Bragg peaks, with real spin-smectic also displaying higher harmonics $\pm n\mathbf{q}_0$ ($n = 2, 3, \dots$). The matrix $D(\mathbf{x})$ above is the magnetic sector correlators defined and calculated in Appendix D, with the trace given by

$$\text{Tr} D(\mathbf{x}) = \begin{cases} e^{-\frac{1}{2} C_{xy,\theta}(\mathbf{x})} - \frac{1}{2} C_{xy,\phi}(\mathbf{x}) & \text{(collinear)}, \\ e^{-\frac{1}{4} C_{xy,\theta}(\mathbf{x})} - \frac{1}{4} C_{xy,\phi}(\mathbf{x}) & \text{(coplanar)}. \end{cases} \quad (113)$$

The key characteristic feature of $\mathcal{S}(\mathbf{q})$ is the 3D quasi-Bragg peak around the ordering wave vector \mathbf{q}_0 . In the above, P_0 is the contributions from short-range correlations that depend smoothly on \mathbf{q} , $P_{\text{sm}}(\mathbf{k})$ is the leading-order singular part due to the quasi-long-range correlation of the smectic phonon, given by ($a = 1$)

$$P_{\text{sm}}(\mathbf{k}) \sim D_0 \begin{cases} \frac{1}{|\mathbf{k}_{\perp}|^{4-2\eta}} & \text{for } k_{\parallel} = 0, \\ \frac{1}{|k_{\parallel}|^{2-\eta}} & \text{for } k_{\perp} = 0, \end{cases} \quad (114)$$

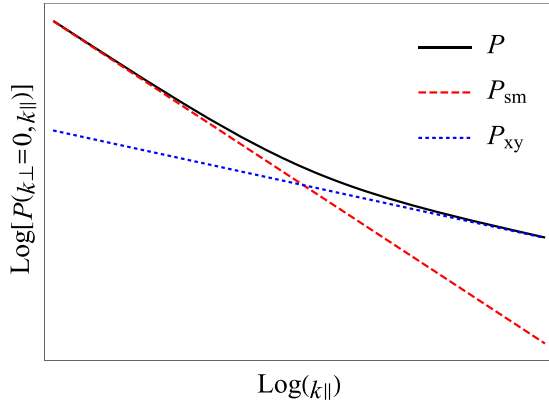


FIG. 6. Schematic plot of the ideal double-power-law peak $P(\mathbf{k}) = P_{\text{sm}}(\mathbf{k}) + P_{\text{xy}}(\mathbf{k})$ in the structure factor along k_{\parallel} . The combined effects of smectic (red-dashed) and XY (blue-dotted) fluctuations give rise to the double-power-law peak (black-solid).

with $D_0 = \text{Tr}D(|\mathbf{x}| \rightarrow \infty)$ the Debye-Waller factor, and $P_{\text{xy}}(\mathbf{k})$ is a subleading singular contribution coming from the power-law dependence in $\text{Tr}D(\mathbf{x})$, (113), which (together with the smectic correlation) is given by

$$P_{\text{xy}}(\mathbf{k}) \sim \frac{T}{\kappa} \begin{cases} \frac{1}{|\mathbf{k}_{\perp}|^{2(1-\eta) + \frac{\eta}{1+\eta}}} & \text{for } k_{\parallel} = 0, \\ \frac{1}{|k_{\parallel}|^{1-\eta + \frac{1}{1+2\eta}}} & \text{for } k_{\perp} = 0, \end{cases} \quad (115)$$

where for simplicity we chose $\kappa = \kappa_{\parallel} = \kappa_{\perp}$, and the nonuniversal temperature-dependent exponent is given by

$$\eta = \frac{q_0^2 T}{16\pi \sqrt{BK}}. \quad (116)$$

As illustrated in Fig. 6, the structure factor exhibits anisotropic ‘‘double-power-law’’ peaks at $\mathbf{q} = \pm \mathbf{q}_0$ with exponents $4 - 2\eta$ and $2 - \eta$ perpendicular and parallel to the ordering wave vector \mathbf{q}_0 , respectively. Away from the peaks, these cross over to $2(1 - \eta) + \frac{\eta}{1+\eta}$ and $1 - \eta + \frac{1}{1+2\eta}$, as dominated by the subleading (but broader) contributions of P_{xy} . The magnitudes of the power-law functions P_{sm} and P_{xy} are nonuniversal, depending on the detailed Goldstone mode dispersions and temperature. In real systems, it may be hard to distinguish the power-law tail of P_{xy} from the nonuniversal contribution P_0 . However, the former may still manifest at high temperatures or small stiffness κ [see Eq. (115)], not only due to the enhanced magnitude of P_{xy} , but also the suppression of P_{sm} by the Debye-Waller factor.

In real crystalline materials, the spin-density waves generally consist of higher harmonics that will also give rise to double-power-law peaks at $\mathbf{q} = \pm n\mathbf{q}_0$ with modified exponents $\eta \rightarrow \eta_n = n^2\eta$; see Eq. (6) and Fig. 2. Furthermore, the spin-density waves tend to form domains with their wave vectors pinned by the underlying lattice. In this case, the structure factor is given by the average of those domain contributions, leading to peaks located on the high symmetry axes of the Brillouin zone. As illustrated in Fig. 7, this also leads to finite-size effects that broaden the power-law contributions P_{sm} and P_{xy} , with the leading singular part P_{sm} by widths $1/\xi^{\text{cr}}$ and $(a_0\xi^{\text{cr}})^{-1/2}$ (ξ^{cr} is the averaged domain size, a_0 is the longest UV scale, within which the smectic dispersion

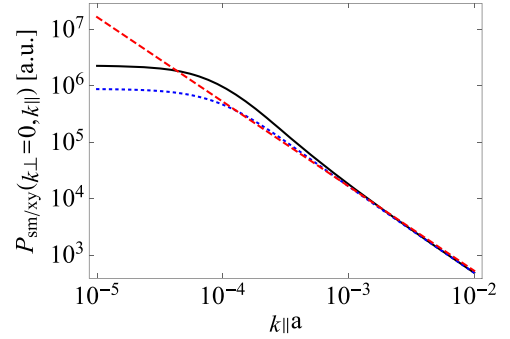


FIG. 7. Schematic plot of the asymptotic behavior of the power-law contribution in the structure factor, $P_{\text{sm}}(\mathbf{k})$ or $P_{\text{xy}}(\mathbf{k})$, along k_{\parallel} . The red-dashed line shows the ideal power-law behavior of $P_{\text{sm/xy}}$ with an exponent 1.5. The blue-dotted curve shows the peak perturbed by an infrared cutoff ξ (chosen to be $10000a$, modeled by an exponential cutoff) due to a finite linear domain size of the system (ξ^{cr} , for P_{sm} or P_{xy}) or SOC effects (ξ^{soc} , only for P_{xy}). The black-solid curve shows the power-law peak P_{sm} perturbed by (in addition to the finite-size cutoff) the lattice anisotropy effects that lead to a crossover scale (chosen to be $\xi/2$) to the XY fluctuations.

starts to deviate) in the parallel and perpendicular directions, respectively.

As shown in Eq. (109), the SOC also gives rise to similar effects on P_{xy} by introducing a gap in the magnetic Goldstone-mode correlators, which terminates the power-law dependence around $\xi_{\parallel/\perp}^{\text{soc}} \approx \sqrt{\kappa_{\parallel/\perp}/k_p}$. For the cases that spins are locked perpendicular to the \mathbf{q}_0 , the collinear and coplanar states have one and two magnetic Goldstone modes gapped, respectively. Accordingly, for the collinear state the asymptotic behaviors of P_{xy} remain the same, while for the coplanar state P_{xy} is broadened by the infrared cutoff introduced by the gap.

In the presence of lattice anisotropy that pins the direction of \mathbf{q}_0 , the smectic correlator becomes long-range-ordered; see Fig. 5. This sharpens the power-law quasi-Bragg peak of P_{sm} to a δ -function Bragg peak, while it modifies the exponents of P_{xy} to be 2. As illustrated in Fig. 7, together with the finite-size effects, this leads to an enhanced peak strength, within the crossover momentum scale (see the black-solid and blue-dotted curves).

Finally, we expect that near a thermal phase transition, the ratio of the spin stiffness $\kappa_{\perp}/\kappa_{\parallel}$ will be small, which can lead to a sizable nonsingular contribution $P_0(\mathbf{q})$ due to strong spin-sector fluctuations, that depend on the ‘‘subleading’’ moduli in (98) and (99) for the collinear and coplanar states, respectively. For the coplanar states, there are strong fluctuations on the spiral surface, which may lead to anisotropic arc-shaped peaks, observed in a classical J_1 - J_2 - J_3 Heisenberg model in Ref. [60].

IV. GINZBURG-LANDAU MODEL

In Sec. II we constructed the spin-density functional designed to give condensation into a spin-smectic state. However, such a functional is unable to capture the nature of a continuous phase transition as its disordered state is an isotropic structureless fluid. Here, we instead construct

a generalized Ginzburg-Landau [$O(N)$ generalization of de Gennes' scalar $N = 1$ model for conventional smectic liquid crystal [11]] model that gives the $O(N)$ smectic as its ordered state and has an additional virtue of describing the continuous transition from the orientationally ordered to the $O(N)$ smectic ordered states.

To this end, we propose the following free-energy density that incorporates the orientation order that is characterized by the wave vector $\hat{\mathbf{q}}$,

$$\begin{aligned} \mathcal{H}_{\text{GL}} = & r|\vec{\psi}|^2 + v_1|\vec{\psi}|^4 + \frac{v_2}{2}|\vec{\psi} \cdot \vec{\psi}|^2 + \frac{J_{\parallel}}{2}|(i\partial_{\parallel} - q_0\delta N_{\parallel})\vec{\psi}|^2 \\ & + \frac{J_{\perp}}{2}|(i\nabla_{\perp} - q_0\delta\mathbf{N}_{\perp})\vec{\psi}|^2 + K_s(\nabla \cdot \delta\mathbf{N})^2 \\ & + K_t(\hat{\mathbf{q}} \cdot \nabla \times \delta\mathbf{N})^2 + K_b(\hat{\mathbf{q}} \times \nabla \times \delta\mathbf{N})^2. \end{aligned} \quad (117)$$

In the above,

$$\delta\mathbf{N}(\mathbf{x}) = \mathbf{N}(\mathbf{x}) - \hat{\mathbf{q}}, \quad \mathbf{N} \cdot \mathbf{N} = 1, \quad (118)$$

are the orientational Goldstone mode fluctuations characterizing the ‘‘nematic’’ phase from which the spin-smectic emerges. As for conventional nematics, they are characterized by the standard Frank-Oseen free energy with the splay (K_s), twist (K_t), and bend (K_b) elastic moduli. The complex vector field, $\vec{\psi}(\mathbf{x}) = \vec{n}(\mathbf{x}) + i\vec{m}(\mathbf{x})$, is the slowly varying order parameter of spin-smectic in (10) that characterizes the strength of spin order (note that \vec{n}, \vec{m} are not unit vectors, with their amplitude growing in the usual Landau way below the transition). As spin-smectic emerges from an anisotropic, orientationally ordered nematic state, the stiffness of the order parameter is anisotropic, $J_{\parallel} \neq J_{\perp}$.

For clarity of presentation, in the following discussion we set $K_t = K_b = K_{tb}$, with the model then simplifying to

$$\begin{aligned} \mathcal{H}_{\text{GL}} = & r|\vec{\psi}|^2 + v_1|\vec{\psi}|^4 + \frac{v_2}{2}|\vec{\psi} \cdot \vec{\psi}|^2 \\ & + \frac{J_{\parallel}}{2}|(i\partial_{\parallel} - q_0\delta N_{\parallel})\vec{\psi}|^2 + \frac{J_{\perp}}{2}|(i\nabla_{\perp} - q_0\delta\mathbf{N}_{\perp})\vec{\psi}|^2 \\ & + K_s(\nabla \cdot \delta\mathbf{N})^2 + K_{tb}(\nabla \times \delta\mathbf{N})^2, \end{aligned} \quad (119)$$

which resembles the Ginzburg-Landau model of a normal-superconductor transition with a nonzero spin-angular momentum pairing (e.g., He3), but with an additional gauge-invariance breaking splay stiffness replacing the Maxwell term for the vector potential.

At high temperatures, $r > 0$, the complex vector field $\vec{\psi}$ is translationally disordered, leaving the Frank-Oseen free energy that describes the nematiclike unidirectional order of the parent liquid state.

At low temperatures, $r < 0$ (and $v_1 > 0$), the spin-smectic order emerges, characterized by a nonzero order parameter,

$$\vec{\psi}(\mathbf{x}) = S_0\hat{\psi}, \quad (120)$$

where for $N = 1$ or $v_2 < 0$, the collinear state that satisfies (18) is energetically preferred with

$$\hat{\psi} = \hat{n}e^{i\chi}, \quad S_0^2 = -r/(2v_1 + v_2). \quad (121)$$

Instead, for $N > 1$ and $v_2 > 0$, the coplanar state that satisfies (22) is more stable with

$$\hat{\psi} = \frac{\hat{n} + i\hat{m}}{\sqrt{2}}, \quad S_0^2 = -r/2v_1. \quad (122)$$

The state is characterized by the coherence length,

$$\xi = \sqrt{\frac{J}{2|r|}}, \quad (123)$$

which governs the spatial distortions of the amplitude $|\vec{\psi}| = S_0$ and thereby the size of the so-called cybotactic clusters near the critical point, and by the orientational ‘‘penetration’’ length

$$\lambda_{tb} = \sqrt{\frac{2K_{tb}}{Jq_0^2S_0^2}}, \quad (124)$$

which is the scale that twist and bend deformation can penetrate through the soft spin-density wave.

Below, we show that at low temperatures this generalized spin-de Gennes model reproduces all the properties of the collinear and coplanar spin-smectic states, but in addition captures the critical properties of the phase transition, whose beyond-mean-field treatment of critical behavior is a challenging problem that we leave to future studies.

A. Collinear state

For the collinear state (121), the coupling terms in (119) become ($\chi = q_0u$)

$$|(i\partial_i - q_0\delta N_i)\hat{\psi}|^2 = (\partial_i\hat{n})^2 + q_0^2(\partial_iu + \delta N_i)^2, \quad (125)$$

where we suspended Einstein's summation convention (no summation over i) and at low temperatures, deep in the collinear spin-smectic state, the minimization of the second term above gives [61] ($\delta N \ll 1$)

$$\delta\mathbf{N}_{\perp} = -\nabla_{\perp}u. \quad (126)$$

This leads to the following low-energy Goldstone theory that describes the collinear state:

$$\begin{aligned} \mathcal{H}_{\text{GL}}^{\text{collinear}} = & \frac{J_{\parallel}S_0^2q_0^2}{2}\left(\partial_{\parallel}u + \frac{(\nabla_{\perp}u)^2}{2}\right)^2 + K_s(\nabla_{\perp}^2u)^2 \\ & + \frac{J_{\parallel}S_0^2}{2}(\partial_{\parallel}\hat{n})^2 + \frac{J_{\perp}S_0^2}{2}(\nabla_{\perp}\hat{n})^2, \end{aligned} \quad (127)$$

in agreement with our earlier analysis in (86) with the identification of the coefficients

$$\frac{J_{\parallel}S_0^2q_0^2}{2} = B, \quad K_s = K, \quad \frac{J_{\parallel/\perp}S_0^2}{2} = \kappa_{\parallel/\perp}, \quad (128)$$

which suggests a divergent anisotropy $J_{\perp}/J_{\parallel} = \kappa_{\perp}/\kappa_{\parallel} \sim S_0^2$ near the critical point, where $S_0 \rightarrow 0$. As before, deep in the phase, here we also neglected the dislocation defects, i.e., $\nabla \times \nabla u = \mathbf{0}$.

B. Coplanar state

For the coplanar spin-smectic state (122), the coupling terms in (119) reduce to

$$\begin{aligned} & |(i\partial_i - q_0\delta N_i)\hat{\psi}|^2 \\ &= |\partial_i\hat{\psi}|^2 - (i\hat{\psi}^* \cdot \partial_i\hat{\psi})^2 + (i\hat{\psi}^* \cdot \partial_i\hat{\psi} - q_0\delta N_i)^2 \\ &= \frac{1}{4}(\partial_i\hat{L})^2 + (\hat{m} \cdot \partial_i\hat{n} - q_0\delta N_i)^2, \end{aligned} \quad (129)$$

where we suspended Einstein's summation convention and in the last line we expressed the out-of-plane fluctuations in terms of $\hat{L}_{\alpha\beta} = \hat{n}_\alpha\hat{m}_\beta - \hat{m}_\alpha\hat{n}_\beta$ using (77).

In the ordered state, the minimization of the second term above gives an emergent Higgs-like mechanism locking orientational and smectic orders according to

$$\delta\mathbf{N}_\perp = \hat{\mathbf{A}}_\perp, \quad (130)$$

where the dimensionless field $\hat{\mathbf{A}} = (\hat{m} \cdot \nabla\hat{n})/q_0$. This then gives the Goldstone mode Hamiltonian for the coplanar state

$$\begin{aligned} \mathcal{H}_{\text{GL}}^{\text{coplanar}} &= \frac{J_\parallel S_0^2 q_0^2}{2} \left(|\hat{\mathbf{A}}_\parallel| - \frac{1}{2}\hat{\mathbf{A}}_\perp^2 \right)^2 \\ &+ K_s(\nabla \cdot \hat{\mathbf{A}}_\perp)^2 + K_{tb}(\nabla \times \hat{\mathbf{A}}_\perp)^2 \\ &+ \frac{J_\parallel S_0^2}{8}(\partial_\parallel\hat{L})^2 + \frac{J_\perp S_0^2}{8}(\nabla_\perp\hat{L})^2, \end{aligned} \quad (131)$$

which reduces to (79) in the absence of dislocations, $\nabla \times \hat{\mathbf{A}}_\perp = \mathbf{0}$, with

$$\frac{J_\parallel S_0^2 q_0^2}{2} = B, \quad K_s = K, \quad \frac{J_{\perp/\parallel} S_0^2}{8} = \kappa_{\perp/\parallel}. \quad (132)$$

This again leads to a divergent anisotropy $J_\perp/J_\parallel \sim S_0^2$ near the critical point, where $S_0 \rightarrow 0$.

As noted above, in addition to reproducing the corresponding spin-smectic states, the spin-de Gennes model faithfully captures the spin-nematic-smectic phase transition that we expect to display rich universal critical phenomenology [62], whose study we leave for the future.

V. QUANTUM DYNAMICS

So far, all of our analysis has been confined to a classical treatment of the spin-smectic states, valid at high temperatures. However, at low temperatures quantum dynamics becomes important, and we need to generalize our model by extending it to include dynamics and quantize it via, e.g., a coherent spin path-integral formulation, following the standard derivation of the conventional antiferromagnetic σ -model with linear dispersion [9,10].

To this end, to capture the zero-temperature dynamics and the associated quantum fluctuations, we now introduce the spin Berry phase that is the Wess-Zumino-Witten action S_{WZW} that encodes the $SU(2)$ ($N=3$) spin commutator algebra into the action, corresponding to spin precession generic to all underdamped spin systems.

To extend this to an array of spins, we sum over lattice sites with the action then given by ($\hbar=1$)

$$\begin{aligned} S_B &= \int dt \dot{\phi}(\mathbf{x}, t)[1 - \cos\theta(\mathbf{x}, t)] \\ &= \int_{\mathbf{x}} S_{\text{WZW}}[\hat{S}(\mathbf{x}, t, u)] \\ &= -s \int_{\mathbf{x}, t} \int_0^1 du \hat{S} \cdot \partial_t \hat{S} \times \partial_u \hat{S}, \end{aligned} \quad (133)$$

where s is the spin magnitude quantum number, $\hat{S}(\mathbf{x}, t, u)$ is the coherent spin label corresponding to orientation of a spins at \mathbf{x} , and auxiliary timelike variable u was introduced to be able to express S_{WZW} covariantly in terms of $\hat{S}(\mathbf{x}, t, u)$, rather than in terms of its polar (θ) and azimuthal (ϕ) angles. It is easy to see that S_{WZW} is a boundary term that after u integral gives the solid angle in (133), swept out by $\hat{S}(\mathbf{x}, t, u)$, which quantizes spin s in integer multiples of $1/2$. This also gives the identification of $\hat{S}(\mathbf{x}, t, u)$ with the physical spin according to $\hat{S}(\mathbf{x}, t, 0) = \hat{S}(\mathbf{x}, t)$ and $\hat{S}(\mathbf{x}, t, 1) = \hat{z}$, with the latter an arbitrary reference spin orientation.

Below, we focus on the coplanar state, expressing \hat{S} in terms of the zero-wave-vector \vec{S}_0 (uniform, ferromagnetic part, not to be confused with the magnitude of spin S_0 in previous sections) and the nonzero wave vector (spiral part) \hat{S}_q contributions,

$$\hat{S} = (\vec{S}_0 + \hat{S}_q)/(1 + 2\vec{S}_0 \cdot \hat{S}_q + \vec{S}_0^2)^{1/2}, \quad (134)$$

where

$$\begin{aligned} \hat{S}_q &= \frac{1}{\sqrt{2}}(\hat{\psi} e^{i\mathbf{q}_0 \cdot \mathbf{x}} + \hat{\psi}^* e^{-i\mathbf{q}_0 \cdot \mathbf{x}}) \\ &= \hat{n} \cos \mathbf{q}_0 \cdot \mathbf{x} + \hat{m} \sin \mathbf{q}_0 \cdot \mathbf{x} \end{aligned} \quad (135)$$

and the denominator is a normalization factor that ensures $\hat{S}^2 = 1$. The uniform component \vec{S}_0 must be included despite being gapped in the spin-spiral state, as it encodes the conserved magnetization and has a nontrivial commutation relation with \hat{S}_q .

We consider small ferromagnetic fluctuations $|\vec{S}_0| \ll 1$ such that

$$\hat{S} \approx \vec{S}_\ell + \hat{S}_q, \quad (136)$$

where $\vec{S}_\ell = \vec{S}_0 - (\vec{S}_0 \cdot \hat{S}_q)\hat{S}_q$ is the components of \vec{S}_0 perpendicular to \hat{S}_q , i.e., $\vec{S}_\ell \parallel \hat{\ell}$. Furthermore, because the ground state is *not* a ferromagnet, uniform magnetization fluctuations \vec{S}_ℓ are gapped, i.e., characterized by a Hamiltonian

$$H_{\text{uniform}} = \frac{1}{2}\gamma^{-1} \int_{\mathbf{x}} \vec{S}_\ell^2, \quad (137)$$

where γ is the uniform ferromagnetic susceptibility in the coplanar state.

With this, the evolution operator is given by ($\hbar=1$)

$$U_t = \int [d\hat{S}(\mathbf{x}, t, u)] e^{iS_B - i \int dt [H_{\text{coplanar}} + H_{\text{uniform}}]}, \quad (138)$$

where H_{coplanar} is given by (68). Inserting the form (136) inside S_B and keeping only linear terms in the gapped uniform

magnetization \vec{S}_ℓ , we find

$$S_B = -s \int_{\mathbf{x},t} \int_0^1 du [\vec{S}_\ell \cdot \partial_t \hat{S}_q \times \partial_u \hat{S}_q + \hat{S}_q \cdot \partial_t \vec{S}_\ell \times \partial_u \hat{S}_q + \hat{S}_q \cdot \partial_t \hat{S}_q \times \partial_u \vec{S}_\ell], \quad (139)$$

where we dropped the term proportional to $\hat{S}_q \cdot \partial_t \hat{S}_q \times \partial_u \hat{S}_q$, which vanishes (for smooth configurations of $\hat{\psi}$) because it oscillates strongly at wave vector \mathbf{q}_0 [63]. The first term above vanishes because it involves three vectors lying in a plane normal to \hat{S}_q . With integration by parts, S_B reduces to a total derivative,

$$\begin{aligned} S_B &= -s \int_{\mathbf{x},t} \int_0^1 du \partial_u (\vec{S}_\ell \cdot \hat{S}_q \times \partial_t \hat{S}_q) \\ &= -s \int_{\mathbf{x},t} \vec{S}_\ell \cdot \hat{S}_q \times \partial_t \hat{S}_q \\ &= -\frac{1}{2} s \int_{\mathbf{x},t} \vec{S}_\ell \cdot (\hat{\psi} \times \partial_t \hat{\psi}^* + \hat{\psi}^* \times \partial_t \hat{\psi}), \end{aligned} \quad (140)$$

where in the last line we dropped the oscillating terms. Integrating over the gapped magnetization field \vec{S}_ℓ and substituting $\hat{\psi} = (\hat{n} + i\hat{m})/\sqrt{2}$, we find

$$\begin{aligned} S_B &= \bar{\gamma} \int dt (\hat{n} \times \partial_t \hat{n} + \hat{m} \times \partial_t \hat{m})^2 \\ &= \bar{\gamma} \int dt [(\partial_t \hat{n})^2 + (\partial_t \hat{m})^2 + 2(\hat{m} \cdot \partial_t \hat{n})^2] \\ &= \bar{\gamma} \int dt [(\partial_t \hat{L})^2 + 4(\hat{m} \cdot \partial_t \hat{n})^2], \end{aligned} \quad (141)$$

where $\bar{\gamma} = s\gamma/2$. This form is straightforwardly generalized to N spin components, and using the identity (77), gives

$$S_B = \bar{\gamma} \int dt \left[\frac{1}{2} (\partial_t \hat{L})^2 + 4(\hat{m} \cdot \partial_t \hat{n})^2 \right], \quad (142)$$

where \hat{L} is defined in (58).

VI. SUMMARY AND CONCLUSION

Motivated by a large number of physical realizations of unidirectional orders in liquid crystals, degenerate atomic gases, electronic, and in particular frustrated magnetic systems, here we developed a low-energy theory of Goldstone modes, i.e., $O(N)$ spin-smectic σ -model that describes unidirectional “density” waves of generalized N -component smectic. We predicted two phases—coplanar and collinear spin-smectics that spontaneously break $O(N)$ -spin and $O(d)$ -spatial rotational symmetries in addition to the translational symmetry along \mathbf{q}_0 [64].

Having established two corresponding $O(N)$ smectic σ -models, we focused on the new physically interesting case of $N = 3$ and examined spin-smectics’ stability to thermal fluctuations within a harmonic approximation. We showed that these states are characterized by a critical dimensions $d_c = 3$ below which the corresponding mean-field order is unstable, to a state with strongly fluctuating Goldstone modes in $d \leq 3$. We briefly discussed the nonlinearities that couple the smectic

and magnetic sectors, reserving their detailed analysis to a future study.

We then used the developed $O(N)$ σ -models to characterize spin-smectic phases by the correlation functions of their Goldstone modes. In addition to the asymptotic behavior of the idealized system, we also discussed the effects of weak symmetry-breaking perturbations that exist in real materials: (i) Lattice anisotropy breaking spatial- $O(d = 3)$ rotational symmetry by pinning \mathbf{q}_0 along high symmetry axes of the underlying lattice, that leads to a smectic to XY model crossover for the smectic phonon mode. (ii) Spin-orbit interaction locking the spin orientation to \mathbf{q}_0 and thereby breaking the $O(N = 3) \times O(d = 3)$ rotational symmetries down to their diagonal subgroup. In particular, for the coplanar state, the spin-plane normal vector $\hat{\ell}$ is frozen along \mathbf{q}_0 , which gaps out the two magnetic Goldstone modes, akin to cholesterics and DM-interacting helical magnets. In materials with weak DM spin-orbit interactions and weak lattice pinning anisotropy compared to the Heisenberg exchange interactions, we predict that spin-smectic σ -models will control the low-temperature Goldstone modes and therefore will exhibit spin-smectic structure function over a large intermediate range of length scales before asymptotically crossing over to a conventional σ -model behavior.

Utilizing these Goldstone modes correlation functions, we computed the static spin structure factors, focusing on their asymptotic long-wavelength behaviors. We showed that at the harmonic level, the $N = 3$ collinear and coplanar spin-smectics are characterized by the same asymptotic form. In 3D they both exhibit double-power-law quasi-Bragg peaks (in contrast to the usual single-power-law for scalar smectics and δ -function Bragg peaks in conventional magnets) at $\pm\mathbf{q}_0$ due to the combined effects of the smectic and XY spin Goldstone mode fluctuations. In addition, we discussed specific applications to magnetic systems, including the effects of various symmetry-breaking perturbations and powder averaging over different spin-smectic domains, that change the asymptotic behaviors of the peaks. However, we expect that even in the ideal case without such perturbations, the double-power-law characteristic feature may be weak, and difficult to distinguish from the nonsingular short-range correlations. Yet, we found that these novel features are enhanced near a phase transition into the spin-nematic state, where the effective transverse to \mathbf{q}_0 spin stiffness vanishes parametrically faster than its longitudinal counterpart. We leave the required detailed analysis near the critical point to future studies.

We also complemented our $O(N)$ spin-smectic σ -model development with a $O(N)$ generalization of a de Gennes–like model that captures the spin-nematic to spin-smectic (NA) phase transition in terms of a complex N -vector order parameter characterizing the spin-smectic state. At the mean-field level, it describes the phase transition and reproduces precisely the $O(N)$ σ -models of the planar and collinear smectic states. However, it raises a challenging question of true criticality of this spin-NA transition, which we leave for future investigations.

An extension of our study to a quantum spin-smectics is another interesting and open direction to explore. Here, by appending our classical theory with the WZW action-spin precessional dynamics, we derived the quantum dynamic for

the coplanar spin state. At the Gaussian level it leads to one smecticlike mode (with linear and quadratic dispersion in the parallel and perpendicular directions, respectively) and $2N - 4$ conventional spin-density-wave-like Goldstone modes with linear dispersion. This allows for the study of the dynamic structure function obtained in neutron scattering, with the analysis left for a future study. Our analysis assumes smooth configurations of spins, and thus neglects possible topological terms that could play a nontrivial role in the properties of spin-smectics. We also leave more detailed studies of this to future research.

Our study is based on an $O(d) \times O(N)$ symmetric field theory, with the discussion of symmetry-breaking effects incorporated phenomenologically. A more microscopic analysis, that allows a quantitative assessment of such symmetry breaking terms, is a necessary next step to assess smectic σ -model applicability and range of validity in real materials.

Other future directions include but are not limited to large- N and RG analyses of the $O(N)$ smectic σ -model, the effects of topological defects, and the generalization of spin-smectic states to different representations of the $O(N) \times O(d)$ group and to other symmetry groups. We hope our study can stimulate future theoretical and experimental studies in such soft spin-density waves and their generalizations.

ACKNOWLEDGMENTS

L.R. thanks John Toner and Arun Paramekanti for enlightening discussions. This research was supported by the Simons Investigator Award to L.R. from the Simons Foundation. L.R. thanks The Kavli Institute for Theoretical Physics for hospitality while this manuscript was in preparation, during Quantum Crystals and Quantum Magnetism workshops, supported by the National Science Foundation under Grants No. NSF PHY-1748958 and No. PHY-2309135.

APPENDIX A: ANALYSIS OF THE GRADIENT TERMS IN THE $O(N)$ SMECTIC MODEL

Here, we evaluate all the symmetry-allowed gradient terms in the field theory (9) up to quartic order in \vec{S} . As discussed in Sec. II, this then leads to universal, low-energy Goldstone mode models for both the collinear and coplanar spin-density wave states. Specifically, we will consider the following quadratic:

$$(\nabla\vec{S})^2, \quad (\nabla^2\vec{S})^2 \quad (\text{A1})$$

and quartic terms

$$(\nabla\vec{S})^4, \quad (\vec{S} \cdot \nabla\vec{S})^2, \quad \sum_{ij} (\partial_i\vec{S} \cdot \partial_j\vec{S})^2. \quad (\text{A2})$$

We note that the important λ_2 term in (9) is the linear combinations of the above terms, given by

$$(\vec{S} \times \nabla\vec{S})^2 = S^2(\nabla\vec{S})^2 - (\vec{S} \cdot \nabla\vec{S})^2. \quad (\text{A3})$$

1. Collinear state

For the collinear state (80) we find ($\chi = qu$),

$$\begin{aligned} \partial_i\vec{S} &= S_0 \text{Re}[(\partial_i\hat{n} + i(\partial_i\chi + q_i)\hat{n})e^{i\mathbf{q}\cdot\mathbf{x}+i\chi}], \\ \partial_i\partial_j\vec{S} &= S_0 \text{Re}[(\partial_i\partial_j\hat{n} - (\partial_i\chi + q_i)(\partial_j\chi + q_j)\hat{n} + i(\partial_i\chi + q_i)\partial_j\hat{n} + i(\partial_j\chi + q_j)\partial_i\hat{n} + i(\partial_i\partial_j\chi)\hat{n}]e^{i\mathbf{q}\cdot\mathbf{x}+i\chi}. \end{aligned} \quad (\text{A4})$$

After dropping the oscillating (in space) contributions (that vanish upon spatial integration), the quadratic terms are given by

$$\begin{aligned} (\nabla\vec{S})^2 &= \frac{S_0^2}{2} [(\nabla\hat{n})^2 + (\nabla\chi + \mathbf{q})^2], \\ (\nabla^2\vec{S})^2 &= \frac{S_0^2}{2} \{(\nabla^2\hat{n})^2 + 2(\nabla\chi + \mathbf{q})^2(\nabla\hat{n})^2 + (\nabla\chi + \mathbf{q})^4 + (\nabla^2\chi)^2 + 4[(\nabla\chi + \mathbf{q}) \cdot \nabla\hat{n}]^2\}, \end{aligned} \quad (\text{A5})$$

where we used $\hat{n} \cdot \nabla^2\hat{n} + (\nabla\hat{n})^2 = 0$. The quartic terms are given by

$$\begin{aligned} S^2(\nabla\vec{S})^2 &= \frac{S_0^4}{8} [3(\nabla\hat{n})^2 + (\nabla\chi + \mathbf{q})^2], \quad (\vec{S} \cdot \nabla\vec{S})^2 = \frac{S_0^4}{8} (\nabla\chi + \mathbf{q})^2, \\ (\nabla\vec{S})^4 &= \frac{S_0^4}{8} [3(\nabla\hat{n})^4 + 3(\nabla\chi + \mathbf{q})^4 + 2(\nabla\chi + \mathbf{q})^2(\nabla\hat{n})^2], \\ (\partial_i\vec{S} \cdot \partial_j\vec{S})^2 &= \frac{S_0^4}{8} \{3(\nabla\hat{n})^4 + 3(\nabla\chi + \mathbf{q})^4 + 2[(\nabla\chi + \mathbf{q}) \cdot \nabla\hat{n}]^2\}. \end{aligned} \quad (\text{A6})$$

We used above expression in the main text to derive the collinear smectic σ -model.

2. Coplanar state

In the coplanar spin-wave state, characterized by the order parameter (49), we instead find

$$\partial_i \vec{S} = S_0 \text{Re}[(\partial_i \hat{\psi} + iq_i \hat{\psi}) e^{i\mathbf{q}\cdot\mathbf{x}}], \quad \partial_i \partial_j \vec{S} = S_0 \text{Re}[(\partial_i \partial_j \hat{\psi} + iq_i \partial_j \hat{\psi} + iq_j \partial_i \hat{\psi} - q_i q_j \hat{\psi}) e^{i\mathbf{q}\cdot\mathbf{x}}], \quad (\text{A7})$$

where $\hat{\psi} = (\hat{n} + i\hat{m})/\sqrt{2}$, with $\hat{n} \cdot \hat{m} = 0$. After dropping the oscillating (in space) terms, the quadratic terms are given by

$$(\nabla \vec{S})^2 = \frac{S_0^2}{2} |\nabla \hat{\psi} + i\mathbf{q} \hat{\psi}|^2, \quad (\nabla^2 \vec{S})^2 = \frac{S_0^2}{2} [|\nabla^2 \hat{\psi} + 2i\mathbf{q} \cdot \nabla \hat{\psi}|^2 + 2q^2 |\nabla \hat{\psi} + i\mathbf{q} \hat{\psi}|^2 - q^4], \quad (\text{A8})$$

where we used the identity $\text{Re}[\hat{\psi}^* \cdot \nabla^2 \hat{\psi}] = -|\nabla \hat{\psi}|^2$. The quartic terms are given by

$$\begin{aligned} (\nabla \vec{S})^4 &= \frac{S_0^4}{4} |\nabla \hat{\psi} + i\mathbf{q} \hat{\psi}|^4 + \frac{S_0^4}{8} |\nabla \hat{\psi} \cdot \nabla \hat{\psi}|^2, \\ (\partial_i \vec{S} \cdot \partial_j \vec{S})^2 &= \frac{S_0^4}{4} \text{Re}[(\partial_i - iq_i) \hat{\psi}^* \cdot (\partial_j + iq_j) \hat{\psi}]^2 + \frac{S_0^4}{8} |\partial_i \hat{\psi} \cdot \partial_j \hat{\psi}|^2, \end{aligned} \quad (\text{A9})$$

and $(\vec{S} \cdot \nabla \vec{S})^2 = 0$ because $S^2 = \text{const}$ for the coplanar state.

In terms of \hat{n} and \hat{m} , the expressions reduce to

$$\begin{aligned} |\nabla \hat{\psi} + i\mathbf{q} \hat{\psi}|^2 &= \frac{1}{2} (\nabla \hat{n} - \mathbf{q} \hat{m})^2 + \frac{1}{2} (\nabla \hat{m} + \mathbf{q} \hat{n})^2, \\ |\nabla^2 \hat{\psi} + 2i\mathbf{q} \cdot \nabla \hat{\psi}|^2 &= \frac{1}{2} (\nabla^2 \hat{n} - 2\mathbf{q} \cdot \nabla \hat{m})^2 + \frac{1}{2} (\nabla^2 \hat{m} + 2\mathbf{q} \cdot \nabla \hat{n})^2, \\ |\partial_i \hat{\psi} \cdot \partial_j \hat{\psi}|^2 &= \frac{1}{4} (\partial_i \hat{n} \cdot \partial_j \hat{n} - \partial_i \hat{m} \cdot \partial_j \hat{m})^2 + \frac{1}{4} (\partial_i \hat{n} \cdot \partial_j \hat{m} + \partial_i \hat{m} \cdot \partial_j \hat{n})^2, \\ \text{Re}[(\partial_i - iq_i) \hat{\psi}^* \cdot (\partial_j + iq_j) \hat{\psi}]^2 &= \left(\frac{1}{2} \partial_i \hat{n} \cdot \partial_j \hat{n} + \frac{1}{2} \partial_i \hat{m} \cdot \partial_j \hat{m} + q_i \hat{m} \cdot \partial_j \hat{n} + q_j \hat{m} \cdot \partial_i \hat{n} + q_i q_j \right)^2. \end{aligned} \quad (\text{A10})$$

APPENDIX B: GAUGE FIELD REPRESENTATION OF THE $O(3)$ COPLANAR σ -MODEL

In this Appendix, we reformulate the coplanar smectic σ -model in terms of gauge (spin-connection) fields constructed from \hat{n} , \hat{m} . For $N = 3$, $\hat{\psi}$, $\hat{\psi}^*$ (or equivalently \hat{n} , \hat{m}) and $\hat{\ell} = \hat{n} \times \hat{m}$ span the spin space:

$$\vec{a} \cdot \vec{b} = (\hat{\psi}^* \cdot \vec{a})(\hat{\psi} \cdot \vec{b}) + (\hat{\psi} \cdot \vec{a})(\hat{\psi}^* \cdot \vec{b}) + (\hat{\ell} \cdot \vec{a})(\hat{\ell} \cdot \vec{b}) = (\hat{n} \cdot \vec{a})(\hat{n} \cdot \vec{b}) + (\hat{m} \cdot \vec{a})(\hat{m} \cdot \vec{b}) + (\hat{\ell} \cdot \vec{a})(\hat{\ell} \cdot \vec{b}). \quad (\text{B1})$$

With this identity, all the terms above can be written in terms of a real vector (in space) field \mathbf{A} and a complex vector field \mathbf{D} , defined by

$$\mathbf{A} = i\hat{\psi}^* \cdot \nabla \hat{\psi}, \quad \mathbf{D} = \hat{\ell} \cdot \nabla \hat{\psi}, \quad (\text{B2})$$

giving

$$\begin{aligned} |\nabla \hat{\psi} + i\mathbf{q} \hat{\psi}|^2 &= |\mathbf{D}|^2 + (\mathbf{A} - \mathbf{q})^2, \\ |\nabla^2 \hat{\psi} + 2i\mathbf{q} \cdot \nabla \hat{\psi}|^2 &= |\mathbf{D} \cdot \mathbf{D}|^2 + (A^2 + |\mathbf{D}|^2)^2 + (\nabla \cdot \mathbf{A})^2 + |(\nabla - i\mathbf{A}) \cdot \mathbf{D}|^2 \\ &\quad + 4\text{Im}[(\mathbf{q} \cdot \mathbf{D}^*)(\nabla - i\mathbf{A}) \cdot \mathbf{D}] - 4(\mathbf{q} \cdot \mathbf{A})(A^2 + |\mathbf{D}|^2) + 4(\mathbf{q} \cdot \mathbf{A})^2 + 4|\mathbf{q} \cdot \mathbf{D}|^2, \\ |\partial_i \hat{\psi} \cdot \partial_j \hat{\psi}|^2 &= |D_i D_j|^2, \\ \text{Re}[(\partial_i - iq_i) \hat{\psi}^* \cdot (\partial_j + iq_j) \hat{\psi}]^2 &= \text{Re}[D_i^* D_j + A_i A_j - q_i A_j - q_j A_i + q_i q_j]^2, \end{aligned} \quad (\text{B3})$$

where we used

$$\begin{aligned} (\partial_i \hat{\psi}) \cdot (\partial_j \hat{\psi}^*) &= (\hat{\psi}^* \cdot \partial_i \hat{\psi})(\hat{\psi} \cdot \partial_j \hat{\psi}^*) + (\hat{\ell} \cdot \partial_i \hat{\psi})(\hat{\ell} \cdot \partial_j \hat{\psi}^*) = A_i A_j + D_i D_j^*, \\ (\partial_i \hat{\psi}) \cdot (\partial_j \hat{\psi}) &= (\hat{\ell} \cdot \partial_i \hat{\psi})(\hat{\ell} \cdot \partial_j \hat{\psi}) = D_i D_j, \\ \hat{\psi}^* \cdot (\nabla^2 \hat{\psi}) &= \partial_i (\hat{\psi}^* \cdot \partial_i \hat{\psi}) - (\nabla \hat{\psi}^*) \cdot (\nabla \hat{\psi}) = -i\nabla \cdot \mathbf{A} - A^2 - |\mathbf{D}|^2, \\ \hat{\psi} \cdot (\nabla^2 \hat{\psi}) &= -(\nabla \hat{\psi})^2 = -D^2, \\ \hat{\ell} \cdot (\nabla^2 \hat{\psi}) &= \partial_i (\hat{\ell} \cdot \partial_i \hat{\psi}) - (\nabla \hat{\ell}) \cdot (\nabla \hat{\psi}) = (\nabla - i\mathbf{A}) \cdot \mathbf{D}. \end{aligned} \quad (\text{B4})$$

We use this description to formulate the coplanar spin-smectic σ -model.

APPENDIX C: COMPLEMENTARY DESCRIPTION OF THE $O(N)$ SMECTIC MODEL AND THE λ_3 TERM

A complementary description of the spin-smectic was proposed by Toner, starting with

$$\mathcal{H}_{\text{Toner}} = J[(\nabla^2 \vec{S})^2 - 2q_0^2(\hat{t} \cdot \nabla \vec{S})^2] + \frac{1}{2}K_0(\nabla \hat{t})^2, \quad (\text{C1})$$

where the nematiclike field \hat{t} ensures underlying rotational symmetry. Using this model to derive Goldstone mode theory for the coplanar state (49), at harmonic level in the small expansion of the orthonormal triad in terms of three angles χ, θ_n, θ_m ,

$$\hat{n} \approx \hat{e}_1 - \chi \hat{e}_2 + \theta_n \hat{e}_3, \quad (\text{C2})$$

$$\hat{m} \approx \hat{e}_2 + \chi \hat{e}_1 + \theta_m \hat{e}_3, \quad (\text{C3})$$

one obtains

$$\mathcal{H}_{\text{Toner}} = \frac{1}{2}B(\partial_z \chi)^2 + \frac{1}{2}K(\nabla_{\perp}^2 \chi)^2 + \frac{1}{2}B(\nabla \theta_n)^2 + \frac{1}{2}B(\nabla \theta_m)^2. \quad (\text{C4})$$

That is, the smectic phonon (spiral phase angle χ) is indeed smecticlike, but the two out-of-plane fluctuations of the triad are XY -like. This form does not exhibit the out-of-plane instability of the ‘‘soft’’ sigma model (53).

This suggests that the first derivation is from a nongeneric model and therefore misses some important couplings that will appear in a more general model. Examination of the model proposed by Toner shows that it contains a new quartic term, which when averaged over \hat{t} gives

$$\langle t_i t_j t_k t_l \rangle (\partial_i \vec{S} \cdot \partial_j \vec{S})(\partial_k \vec{S} \cdot \partial_l \vec{S}) \propto |\nabla \vec{S}|^4 + 2(\partial_i \vec{S} \cdot \partial_j \vec{S})^2, \quad (\text{C5})$$

where we used isotropy of the \hat{t} probability distribution. The second term is the stabilizing λ_3 quartic term that enters crucially for the nonlinear planar spin-smectic σ -model.

APPENDIX D: CALCULATION DETAILS OF THE SPIN-SMECTIC STRUCTURE FACTOR

In this Appendix, we calculate the spin-smectic structure factor in a Gaussian approximation using the angular representation of the spin-density waves in Sec. III A. We note that the analysis below neglects the effects of nonlinearities that may lead to a crossover to a nontrivial spin-smectic fixed point, thereby modifying these predictions at long scales. We first calculate thermal averages of the Goldstone modes, $\varphi, \varphi' = \chi, \theta, \phi$ (or superposition of them):

$$\begin{aligned} \langle \cos \varphi \rangle &= \frac{1}{2} \langle e^{i\varphi} \rangle + \frac{1}{2} \langle e^{-i\varphi} \rangle = \frac{1}{2} e^{-\frac{1}{2} \langle \varphi^2 \rangle} + \frac{1}{2} e^{-\frac{1}{2} \langle \varphi^2 \rangle} = e^{-\frac{1}{2} \langle \varphi^2 \rangle}, \\ \langle \sin \varphi \rangle &= \frac{1}{2i} \langle e^{i\varphi} \rangle - \frac{1}{2i} \langle e^{-i\varphi} \rangle = \frac{1}{2i} e^{-\frac{1}{2} \langle \varphi^2 \rangle} - \frac{1}{2i} e^{-\frac{1}{2} \langle \varphi^2 \rangle} = 0. \end{aligned} \quad (\text{D1})$$

Accordingly the following two-point correlators are given by:

$$\begin{aligned} \langle \cos \varphi(\mathbf{x}) \cos \varphi'(\mathbf{x}') \rangle &= \frac{1}{2} \langle \cos[\varphi(\mathbf{x}) + \varphi'(\mathbf{x}')] \rangle + \frac{1}{2} \langle \cos[\varphi(\mathbf{x}) - \varphi'(\mathbf{x}')] \rangle = e^{-\frac{1}{2} \langle \varphi^2 \rangle - \frac{1}{2} \langle \varphi'^2 \rangle} \cosh C_{\varphi\varphi'}(\mathbf{x} - \mathbf{x}'), \\ \langle \sin \varphi(\mathbf{x}) \sin \varphi'(\mathbf{x}') \rangle &= \frac{1}{2} \langle \cos[\varphi(\mathbf{x}) - \varphi'(\mathbf{x}')] \rangle - \frac{1}{2} \langle \cos[\varphi(\mathbf{x}) + \varphi'(\mathbf{x}')] \rangle = e^{-\frac{1}{2} \langle \varphi^2 \rangle - \frac{1}{2} \langle \varphi'^2 \rangle} \sinh C_{\varphi\varphi'}(\mathbf{x} - \mathbf{x}'), \\ \langle \cos \varphi(\mathbf{x}) \sin \varphi'(\mathbf{x}') \rangle &= \frac{1}{2} \langle \sin[\varphi(\mathbf{x}) + \varphi'(\mathbf{x}')] \rangle - \frac{1}{2} \langle \sin[\varphi(\mathbf{x}) - \varphi'(\mathbf{x}')] \rangle = 0, \end{aligned} \quad (\text{D2})$$

where

$$C_{\varphi\varphi'}(\mathbf{x} - \mathbf{x}') = \langle \varphi(\mathbf{x}) \varphi'(\mathbf{x}') \rangle. \quad (\text{D3})$$

In general, all Goldstone modes are coupled and therefore $C_{\varphi\varphi'} \neq 0$ for any φ and φ' . Below, we neglect the coupling between θ, ϕ , and χ , a valid approximation at low energies. Specifically, we consider the correlators

$$C_{\chi\chi}(\mathbf{x}), \quad C_{\theta\theta}(\mathbf{x}), \quad C_{\phi\phi}(\mathbf{x}), \quad (\text{D4})$$

neglecting all others. The structure factor $\mathcal{S}(\mathbf{q})$ is given by the Fourier transform of the spin-spin correlation function, (110).

1. Collinear state

For the collinear state (80), the spin-spin correlation function in momentum space is given by

$$\begin{aligned} \int_{\mathbf{x}, \mathbf{x}'} e^{i\mathbf{q} \cdot (\mathbf{x} - \mathbf{x}')} \langle S_{\alpha}(\mathbf{x}) S_{\beta}(\mathbf{x}') \rangle &= \int_{\mathbf{x}, \mathbf{x}'} e^{i\mathbf{q} \cdot (\mathbf{x} - \mathbf{x}')} \langle \hat{n}_{\alpha}(\mathbf{x}) \hat{n}_{\beta}(\mathbf{x}') \rangle \langle \cos[\mathbf{q}_0 \cdot \mathbf{x} + \chi(\mathbf{x})] \cos[\mathbf{q}_0 \cdot \mathbf{x}' + \chi(\mathbf{x}')] \rangle \\ &= \frac{V}{4} \int_{\mathbf{x}} [e^{i(\mathbf{q} - \mathbf{q}_0) \cdot \mathbf{x}} + e^{i(\mathbf{q} + \mathbf{q}_0) \cdot \mathbf{x}}] D_{\alpha\beta}(\mathbf{x}) e^{-\frac{1}{2} q_0^2 C_{\text{sm}}(\mathbf{x})}, \end{aligned} \quad (\text{D5})$$

where in the second line above we dropped the term proportional to $e^{\pm i\mathbf{q}\cdot(\mathbf{x}+\mathbf{x}')}$ that will average to zero for $\mathbf{q}_0 \neq \mathbf{0}$ and then renamed $\mathbf{x} - \mathbf{x}' \rightarrow \mathbf{x}$. In the above, $C_{\text{sm}}(\mathbf{x})$ is defined in (105) and $D_{\alpha\beta}(\mathbf{x}) = \langle \hat{n}_\alpha(\mathbf{x}) \hat{n}_\beta(0) \rangle$, where by using (90) the matrix elements are given by

$$D_{11} = e^{-(\theta^2) - \langle \phi^2 \rangle} \cosh C_{\theta\theta}(\mathbf{x}) \cosh C_{\phi\phi}(\mathbf{x}), \quad D_{22} = \frac{1}{2} e^{-(\theta^2) - \langle \phi^2 \rangle} \cosh C_{\theta\theta}(\mathbf{x}) \sinh C_{\phi\phi}(\mathbf{x}), \quad D_{33} = e^{-(\theta^2)} \sinh C_{\theta\theta}(\mathbf{x}), \quad (D6)$$

and all others vanish. Keeping terms up to quadratic order in Goldstone modes, we have

$$D(\mathbf{x}) \approx \begin{pmatrix} 1 - \langle \theta^2 \rangle - \langle \phi^2 \rangle & 0 & 0 \\ 0 & C_{\phi\phi}(\mathbf{x}) & 0 \\ 0 & 0 & C_{\theta\theta}(\mathbf{x}) \end{pmatrix}. \quad (D7)$$

This harmonic approximation is consistent with the one we made on the Hamiltonian and it gives the physically reasonable expression that is symmetric around the axis \hat{e}_1 , i.e., $D_{22} = D_{33}$. Within this Gaussian approximation, the structure factor is then given by

$$\begin{aligned} S(\mathbf{q}) &= \frac{1}{V} \sum_{\alpha} \int_{\mathbf{x}, \mathbf{x}'} e^{i\mathbf{q}\cdot(\mathbf{x}-\mathbf{x}')} \langle S_{\alpha}(\mathbf{x}) S_{\alpha}(\mathbf{x}') \rangle, \\ &\approx \frac{1}{4} \int_{\mathbf{x}} [e^{i(\mathbf{q}-\mathbf{q}_0)\cdot\mathbf{x}} + e^{i(\mathbf{q}+\mathbf{q}_0)\cdot\mathbf{x}}] e^{-\frac{1}{2}q_0^2 C_{\text{sm}}(\mathbf{x}) - \frac{1}{2}C_{xy,\theta}(\mathbf{x}) - \frac{1}{2}C_{xy,\phi}(\mathbf{x})}, \end{aligned} \quad (D8)$$

where $C_{xy,\theta}(\mathbf{x})$ and $C_{xy,\phi}(\mathbf{x})$ are defined in (107), and in the last line we rewrote small Goldstone mode fluctuations in an exponential form, $\text{Tr}D(\mathbf{x}) = e^{-\frac{1}{2}C_{xy,\theta}(\mathbf{x}) - \frac{1}{2}C_{xy,\phi}(\mathbf{x})}$.

2. Coplanar state

Repeating the above analysis and approximations for the coplanar state (49), the spin-spin correlation function in momentum space is then given by

$$\begin{aligned} \int_{\mathbf{x}, \mathbf{x}'} e^{i\mathbf{q}\cdot(\mathbf{x}-\mathbf{x}')} \langle S_{\alpha}(\mathbf{x}) S_{\beta}(\mathbf{x}') \rangle &= \frac{1}{4} \int_{\mathbf{x}, \mathbf{x}'} e^{i\mathbf{q}\cdot(\mathbf{x}-\mathbf{x}')} (\langle \hat{\psi}_{\alpha}(\mathbf{x}) \hat{\psi}_{\beta}^*(\mathbf{x}') \rangle e^{i\mathbf{q}_0\cdot(\mathbf{x}-\mathbf{x}')} + \langle \hat{\psi}_{\alpha}(\mathbf{x}) \hat{\psi}_{\beta}(\mathbf{x}') \rangle e^{i\mathbf{q}_0\cdot(\mathbf{x}+\mathbf{x}')} + \text{H.c.}) \\ &= \frac{V}{4} \int_{\mathbf{x}} [e^{i(\mathbf{q}+\mathbf{q}_0)\cdot\mathbf{x}} D_{\alpha\beta}(\mathbf{x}) + e^{i(\mathbf{q}-\mathbf{q}_0)\cdot\mathbf{x}} D_{\alpha\beta}^*(\mathbf{x})] e^{-\frac{1}{2}q_0^2 C_{\text{sm}}(\mathbf{x})}, \end{aligned} \quad (D9)$$

where $D_{\alpha\beta}(\mathbf{x}) = \langle \hat{\psi}_{\alpha}(\mathbf{x}) \hat{\psi}_{\beta}^*(0) e^{i[\chi(\mathbf{x}) - \chi(0)]} \rangle$ and H.c. denotes the Hermitian conjugate. Using (93), the matrix elements are given by

$$\begin{aligned} D_{11} &= \frac{1}{2} e^{-(\theta^2) - \langle \phi^2 \rangle} \sinh C_{\theta\theta}(\mathbf{x}) \cosh C_{\phi\phi}(\mathbf{x}) + \frac{1}{2} e^{-\langle \phi^2 \rangle} \sinh C_{\phi\phi}(\mathbf{x}), \\ D_{22} &= \frac{1}{2} e^{-(\theta^2) - \langle \phi^2 \rangle} \sinh C_{\theta\theta}(\mathbf{x}) \sinh C_{\phi\phi}(\mathbf{x}) + \frac{1}{2} e^{-\langle \phi^2 \rangle} \cosh C_{\phi\phi}(\mathbf{x}), \\ D_{33} &= \frac{1}{2} e^{-(\theta^2)} \cosh C_{\theta\theta}(\mathbf{x}), \quad D_{32} = -D_{23} = \frac{i}{2} e^{-\frac{1}{2}(\theta^2) - \frac{1}{2}\langle \phi^2 \rangle}, \end{aligned} \quad (D10)$$

with all others contributions vanishing. For small Goldstone mode fluctuations, we obtain a physically reasonable expression that is symmetric around the \hat{e}_1 axis,

$$D \approx \frac{1}{2} \begin{pmatrix} C_{\theta\theta}(\mathbf{x}) + C_{\phi\phi}(\mathbf{x}) & 0 & 0 \\ 0 & 1 - \langle \phi^2 \rangle & -i(1 - \frac{1}{2}\langle \theta^2 \rangle - \frac{1}{2}\langle \phi^2 \rangle) \\ 0 & i(1 - \frac{1}{2}\langle \theta^2 \rangle - \frac{1}{2}\langle \phi^2 \rangle) & 1 - \langle \theta^2 \rangle \end{pmatrix}. \quad (D11)$$

With these approximations, the structure factor is then given by

$$\begin{aligned} S(\mathbf{q}) &= \frac{1}{V} \sum_{\alpha} \int_{\mathbf{x}, \mathbf{x}'} e^{i\mathbf{q}\cdot(\mathbf{x}-\mathbf{x}')} \langle S_{\alpha}(\mathbf{x}) S_{\alpha}(\mathbf{x}') \rangle \\ &= \frac{1}{4} \sum_{\alpha} \int_{\mathbf{x}} [e^{i(\mathbf{q}-\mathbf{q}_0)\cdot\mathbf{x}} + e^{i(\mathbf{q}+\mathbf{q}_0)\cdot\mathbf{x}}] D_{\alpha\alpha}(\mathbf{x}) e^{-\frac{1}{2}q_0^2 C_{\text{sm}}(\mathbf{x})} \\ &\approx \frac{1}{4} \int_{\mathbf{x}} [e^{i(\mathbf{q}-\mathbf{q}_0)\cdot\mathbf{x}} + e^{i(\mathbf{q}+\mathbf{q}_0)\cdot\mathbf{x}}] e^{-\frac{1}{2}q_0^2 C_{\text{sm}}(\mathbf{x}) - \frac{1}{4}C_{xy,\theta}(\mathbf{x}) - \frac{1}{4}C_{xy,\phi}(\mathbf{x})}, \end{aligned} \quad (D12)$$

where in the last line we rewrote the small Goldstone mode fluctuations in exponential form, $\text{Tr}D(\mathbf{x}) = e^{-\frac{1}{4}C_{xy,\theta}(\mathbf{x}) - \frac{1}{4}C_{xy,\phi}(\mathbf{x})}$.

The expressions for the collinear (D8) and coplanar (D12) structure factors, together with the Goldstone mode correlators (105) and (107), lead to the same asymptotic form (111), characterized by the following double-power-law peaks:

$$P(\mathbf{k}) = P_{\text{sm}}(\mathbf{k}) + P_{xy}(\mathbf{k}). \quad (\text{D13})$$

In the above, the leading power-law contribution is from the smectic Goldstone mode fluctuations, given by

$$\begin{aligned} P_{\text{sm}}(\mathbf{k}) &= D_0 \int_{|\mathbf{x}| \gg a} e^{i\mathbf{k}\cdot\mathbf{x}} e^{-\frac{1}{2}q_0^2 C_{\text{sm}}(\mathbf{x})} \\ &\sim D_0 \int dx_{\parallel} d^2x_{\perp} e^{i\mathbf{k}\cdot\mathbf{x}} \times \begin{cases} \frac{1}{x_{\perp}^{2\eta}} & \text{for } x_{\perp} \gg \sqrt{\lambda|x_{\parallel}|}, \\ \frac{1}{x_{\parallel}^{\eta}} & \text{for } x_{\perp} \ll \sqrt{\lambda|x_{\parallel}|}, \end{cases} \\ &\sim D_0 \begin{cases} \frac{1}{|k_{\perp}|^{4-2\eta}} & \text{for } k_{\parallel} = 0, \\ \frac{1}{|k_{\parallel}|^{2-\eta}} & \text{for } k_{\perp} = 0, \end{cases} \end{aligned} \quad (\text{D14})$$

where $D_0 = \text{Tr}D(x \rightarrow \infty)$ is the Debye-Waller factor, the temperature-dependent exponent η is given by (116), and we used the change of variable $x_{\parallel} = x_{\perp}^2$ to get the last line. On the other hand, the subleading power-law contribution is a consequence of the combined effects of the smectic and XY Goldstone mode fluctuations, given by

$$\begin{aligned} P_{xy}(\mathbf{k}) &\sim \int_{|\mathbf{x}| \gg a} e^{i\mathbf{k}\cdot\mathbf{x}} e^{-\frac{1}{2}q_0^2 C_{\text{sm}}(\mathbf{x})} [C_{\theta\theta}(\mathbf{x}) + C_{\phi\phi}(\mathbf{x})] \\ &\sim \frac{T}{\kappa} \int dx_{\parallel} d^2x_{\perp} e^{i\mathbf{k}\cdot\mathbf{x}} \times \begin{cases} \frac{1}{x_{\perp}^{2\eta+1}} & \text{for } x_{\perp} \gg \sqrt{\lambda|x_{\parallel}|}, \\ \frac{1}{x_{\parallel}^{\eta+1}} & \text{for } x_{\perp} \ll \sqrt{\lambda|x_{\parallel}|}, \end{cases} \\ &\sim \frac{T}{\kappa} \begin{cases} \frac{1}{|k_{\perp}|^{2(1-\eta)+\frac{\eta}{1+\eta}}} & \text{for } k_{\parallel} = 0, \\ \frac{1}{|k_{\parallel}|^{1-\eta+\frac{1}{1+2\eta}}} & \text{for } k_{\perp} = 0, \end{cases} \end{aligned} \quad (\text{D15})$$

where for simplicity we chose $\kappa = \kappa_{\parallel} = \kappa_{\perp}$ and we used the change of variable $x_{\parallel}^{\eta+1} = x_{\perp}^{2\eta+1}$ to get the last line.

-
- [1] Throughout the manuscript, we will use the term ‘‘density’’ to also refer to spin, Cooper pair, and other generalized densities that transform nontrivially under internal symmetry.
- [2] S. Chakravarty, B. I. Halperin, and D. R. Nelson, Two-dimensional quantum Heisenberg antiferromagnet at low temperatures, *Phys. Rev. B* **39**, 2344 (1989).
- [3] P. A. Lee and T. M. Rice, Electric field depinning of charge density waves, *Phys. Rev. B* **19**, 3970 (1979).
- [4] E. Wigner, On the interaction of electrons in metals, *Phys. Rev.* **46**, 1002 (1934).
- [5] D. F. Agterberg, J. S. Davis, S. D. Edkins, E. Fradkin, D. J. Van Harlingen, S. A. Kivelson, P. A. Lee, L. Radzihovsky, J. M. Tranquada, and Y. Wang, The physics of pair-density waves: Cuprate superconductors and beyond, *Annu. Rev. Condens. Matter Phys.* **11**, 231 (2020).
- [6] A. M. Polyakov, Interaction of goldstone particles in two dimensions. Applications to ferromagnets and massive Yang-Mills fields, *Phys. Lett. B* **59**, 79 (1975).
- [7] D. R. Nelson and R. A. Pelcovits, Momentum-shell recursion relations, anisotropic spins, and liquid crystals in $2 + \epsilon$ dimensions, *Phys. Rev. B* **16**, 2191 (1977).
- [8] F. D. M. Haldane, Nonlinear field theory of large-spin Heisenberg antiferromagnets: Semiclassically quantized solitons of the one-dimensional easy-axis Néel state, *Phys. Rev. Lett.* **50**, 1153 (1983).
- [9] F. D. M. Haldane, O(3) nonlinear σ model and the topological distinction between integer- and half-integer-spin antiferromagnets in two dimensions, *Phys. Rev. Lett.* **61**, 1029 (1988).
- [10] T. Dombre and N. Read, Nonlinear σ models for triangular quantum antiferromagnets, *Phys. Rev. B* **39**, 6797 (1989).
- [11] P. G. de Gennes and J. Prost, *The Physics of Liquid Crystals*, 2nd ed. (Clarendon Press, Oxford, 1995).
- [12] G. Grinstein and R. A. Pelcovits, Anharmonic effects in bulk smectic liquid crystals and other ‘‘one-dimensional solids,’’ *Phys. Rev. Lett.* **47**, 856 (1981).
- [13] G. Grinstein and R. A. Pelcovits, Nonlinear elastic theory of smectic liquid crystals, *Phys. Rev. A* **26**, 915 (1982).
- [14] L. Radzihovsky and J. Toner, Nematic-to-smectic-A transition in aerogel, *Phys. Rev. Lett.* **79**, 4214 (1997).
- [15] L. Radzihovsky and J. Toner, Smectic liquid crystals in random environments, *Phys. Rev. B* **60**, 206 (1999).
- [16] T. Bellini, L. Radzihovsky, J. Toner, and N. A. Clark, Universality and scaling in the disordering of a smectic liquid crystal, *Science* **294**, 1074 (2001).
- [17] A. Aharony, O. Entin-Wohlman, D. A. Huse, and L. Radzihovsky, *50 Years of the Renormalization Group*, (World Scientific, Singapore, 2024).
- [18] M. P. Lilly, K. B. Cooper, J. P. Eisenstein, L. N. Pfeiffer, and K. W. West, Evidence for an anisotropic state of

- two-dimensional electrons in high Landau levels, *Phys. Rev. Lett.* **82**, 394 (1999).
- [19] A. A. Koulakov, M. M. Fogler, and B. I. Shklovskii, Charge density wave in two-dimensional electron liquid in weak magnetic field, *Phys. Rev. Lett.* **76**, 499 (1996).
- [20] R. Moessner and J. T. Chalker, Exact results for interacting electrons in high Landau levels, *Phys. Rev. B* **54**, 5006 (1996).
- [21] E. Fradkin and S. A. Kivelson, Liquid-crystal phases of quantum Hall systems, *Phys. Rev. B* **59**, 8065 (1999).
- [22] A. H. MacDonald and M. P. A. Fisher, Quantum theory of quantum Hall smectics, *Phys. Rev. B* **61**, 5724 (2000).
- [23] L. Radzihovsky and A. T. Dorsey, Theory of quantum Hall nematics, *Phys. Rev. Lett.* **88**, 216802 (2002).
- [24] L. Radzihovsky and T. C. Lubensky, Nonlinear smectic elasticity of helical state in cholesteric liquid crystals and helimagnets, *Phys. Rev. E* **83**, 051701 (2011).
- [25] H. Zhai, Degenerate quantum gases with spin-orbit coupling: A review, *Rep. Prog. Phys.* **78**, 026001 (2015).
- [26] L. Tanzi, S. M. Roccuzzo, E. Lucioni, F. Famà, A. Fioretti, C. Gabbanini, G. Modugno, A. Recati, and S. Stringari, Supersolid symmetry breaking from compressional oscillations in a dipolar quantum gas, *Nature (London)* **574**, 382 (2019).
- [27] P. Fulde and R. A. Ferrell, Superconductivity in a strong spin-exchange field, *Phys. Rev.* **135**, A550 (1964).
- [28] A. I. Larkin and Y. N. Ovchinnikov, Nonuniform state of superconductors, *Zh. Eksp. Teor. Fiz.* **47**, 1136 (1964).
- [29] L. Radzihovsky and A. Vishwanath, Quantum liquid crystals in an imbalanced Fermi gas: Fluctuations and fractional vortices in Larkin-Ovchinnikov states, *Phys. Rev. Lett.* **103**, 010404 (2009).
- [30] L. Radzihovsky, Fluctuations and phase transitions in Larkin-Ovchinnikov liquid-crystal states of a population-imbalanced resonant Fermi gas, *Phys. Rev. A* **84**, 023611 (2011).
- [31] L. Radzihovsky and S. Choi, p -wave resonant Bose gas: A finite-momentum spinor superfluid, *Phys. Rev. Lett.* **103**, 095302 (2009).
- [32] S. Choi and L. Radzihovsky, Finite-momentum superfluidity and phase transitions in a p -wave resonant Bose gas, *Phys. Rev. A* **84**, 043612 (2011).
- [33] T.-C. Hsieh, H. Ma, and L. Radzihovsky, Helical superfluid in a frustrated honeycomb Bose-Hubbard model, *Phys. Rev. A* **106**, 023321 (2022).
- [34] These are distinct from another interesting class of helimagnets arising from the chiral Dzyaloshinskii-Moriya (DM) spin-orbit interaction that drives the helical structure. Such DM helical states are less symmetrical than those considered in this paper, and they do *not* exhibit independent $O(N)$ and $O(d)$ symmetries. In such systems, equivalent to a cholesteric liquid crystal, the orientations of \mathbf{q}_0 and \vec{S} are locked, and thus at low energies its Goldstone mode reduces to that of a smectic, as discussed in Ref. [24]. Physical realizations of such system include MnSi, which is an itinerant ferromagnet exhibiting helical structure at low temperatures. These systems show anomalous magnetic [50–52] and transport [53] behavior as probed over different temperature, pressure, and magnetic field.
- [35] D. Bergman, J. Alicea, E. Gull, S. Trebst, and L. Balents, Order-by-disorder and spiral spin-liquid in frustrated diamond-lattice antiferromagnets, *Nat. Phys.* **3**, 487 (2007).
- [36] A. Mulder, R. Ganesh, L. Capriotti, and A. Paramekanti, Spiral order by disorder and lattice nematic order in a frustrated Heisenberg antiferromagnet on the honeycomb lattice, *Phys. Rev. B* **81**, 214419 (2010).
- [37] N. Tristan, J. Hemberger, A. Krimmel, H.-A. Krug von Nidda, V. Tsurkan, and A. Loidl, Geometric frustration in the cubic spinels MAl_2O_4 ($\text{M} = \text{Co}, \text{Fe}, \text{and Mn}$), *Phys. Rev. B* **72**, 174404 (2005).
- [38] T. Suzuki, H. Nagai, M. Nohara, and H. Takagi, Melting of antiferromagnetic ordering in spinel oxide CoAl_2O_4 , *J. Phys.: Condens. Matter* **19**, 145265 (2007).
- [39] V. Fritsch, J. Hemberger, N. Büttgen, E.-W. Scheidt, H.-A. Krug von Nidda, A. Loidl, and V. Tsurkan, Spin and orbital frustration in MnSc_2S_4 and FeSc_2S_4 , *Phys. Rev. Lett.* **92**, 116401 (2004).
- [40] S. Gao, M. A. McGuire, Y. Liu, D. L. Abernathy, C. dela Cruz, M. Frontzek, M. B. Stone, and A. D. Christianson, Spiral spin liquid on a honeycomb lattice, *Phys. Rev. Lett.* **128**, 227201 (2022).
- [41] M. M. Bordelon, C. Liu, L. Posthuma, E. Kenney, M. J. Graf, N. P. Butch, A. Banerjee, S. Calder, L. Balents, and S. D. Wilson, Frustrated Heisenberg $J_1 - J_2$ model within the stretched diamond lattice of LiYbO_2 , *Phys. Rev. B* **103**, 014420 (2021).
- [42] A. P. Ramirez, Strongly geometrically frustrated magnets, *Annu. Rev. Mater. Sci.* **24**, 453 (1994).
- [43] L. Balents, Spin liquids in frustrated magnets, *Nature (London)* **464**, 199 (2010).
- [44] J. Villain, R. Bidaux, J.-P. Carton, and R. Conte, Order as an effect of disorder, *J. Phys.* **41**, 1263 (1980).
- [45] C. L. Henley, Ordering due to disorder in a frustrated vector antiferromagnet, *Phys. Rev. Lett.* **62**, 2056 (1989).
- [46] Generally, the wave vector that minimizes the energy $|\mathbf{q}| = q_0 \neq \bar{q}_0$, as it can be corrected by other (than J) gradient terms and higher-order fluctuations.
- [47] We do not consider multi- \mathbf{q} , nor non-Landau spin liquid states [43]. Determining the true ground state among the single- \mathbf{q} and these states is a challenging microscopic question that falls outside of effective field theory approach taken here and is best addressed numerically.
- [48] On this account, higher-order gradient quartic-in- \vec{S} terms can be included, but add nothing new beyond those already included in (9), which is the minimum form required for a generic description, as we verify *a posteriori*.
- [49] Alternatively, we can consider N orthonormal basis vectors of the spin space: \hat{n} , \hat{m} , and $\{\hat{\ell}^\alpha\}$ ($\alpha = 1, \dots, N - 2$). The generators of rotation that act on the orthonormal diad correspond to the $\hat{n} - \hat{m}$, $\hat{n} - \hat{\ell}^\alpha$, and $\hat{m} - \hat{\ell}^\alpha$ planes. This then leads to $1 + (N - 2) + (N - 2) = 2N - 3$ Goldstone modes that live on the compact $S_{N-1} \times S_{N-2}$ manifold, with S_{N-1} and S_{N-2} (for a given choice) corresponding to the rotations of $\{\hat{n} - \hat{m}, \hat{n} - \hat{\ell}^\alpha\}$ and $\{\hat{m} - \hat{\ell}^\alpha\}$, respectively.
- [50] C. Pfleiderer, D. Reznik, L. Pintschovius, H. v Löhneysen, M. Garst, and A. Rosch, Partial order in the non-Fermi-liquid phase of MnSi, *Nature (London)* **427**, 227 (2004).
- [51] S. V. Grigoriev, S. V. Maleyev, A. I. Okorokov, Yu. O. Chetverikov, R. Georgii, P. Böni, D. Lamago, H. Eckerlebe, and K. Pranzas, Critical fluctuations in MnSi near T_C : A polarized neutron scattering study, *Phys. Rev. B* **72**, 134420 (2005).
- [52] S. Mühlbauer, B. Binz, F. Jonietz, C. Pfleiderer, A. Rosch, A. Neubauer, R. Georgii, and P. Böni, Skyrmion lattice in a chiral magnet, *Science* **323**, 915 (2009).

- [53] A. Neubauer, C. Pfleiderer, B. Binz, A. Rosch, R. Ritz, P. G. Niklowitz, and P. Böni, Topological Hall effect in the A Phase of MnSi, *Phys. Rev. Lett.* **102**, 186602 (2009).
- [54] N. D. Mermin and H. Wagner, Absence of ferromagnetism or antiferromagnetism in one- or two-dimensional isotropic Heisenberg models, *Phys. Rev. Lett.* **17**, 1133 (1966).
- [55] P. C. Hohenberg, Existence of long-range order in one and two dimensions, *Phys. Rev.* **158**, 383 (1967).
- [56] A. Caillé, Remarks on the scattering of X-rays by A-type smectics, *C.R. Seances Acad. Sci. Ser. B* **274**, 891 (1972).
- [57] L. Golubović and Z.-G. Wang, Anharmonic elasticity of smectics A and the Kardar-Parisi-Zhang model, *Phys. Rev. Lett.* **69**, 2535 (1992).
- [58] At the critical dimension $d = 3$, $g^* = 0$, the smectic is in principle described by a Gaussian fixed point, but with logarithmic corrections to the correlation functions and physical observables due to marginally irrelevant flows [12,13] akin to the Ising model at $d = 4$.
- [59] J. Toner and D. R. Nelson, Smectic, cholesteric, and Rayleigh-Benard order in two dimensions, *Phys. Rev. B* **23**, 316 (1981).
- [60] C. Glittum and O. F. Syljuåsen, Arc-shaped structure factor in the J_1 - J_2 - J_3 classical heisenberg model on the triangular lattice, *Phys. Rev. B* **104**, 184427 (2021).
- [61] This can be done exactly using a Lagrangian multiplier to impose the constraint $\mathbf{N} \cdot \mathbf{N} = 1$. See, e.g., Ref. [24].
- [62] B. I. Halperin, T. C. Lubensky, and S.-K. Ma, First-order phase transitions in superconductors and smectic-A liquid crystals, *Phys. Rev. Lett.* **32**, 292 (1974).
- [63] This can, however, lead to nontrivial topological contributions that, e.g., for $d = 1$ leads to the distinction between integer and half-integer spins in Heisenberg antiferromagnets [8].
- [64] Strictly speaking, the coplanar smectic state does *not* break translational symmetry. Instead it breaks the tensor product of translations along and rotations around the ordering wave vector \mathbf{q}_0 down to their diagonal subgroup, namely $U_{\text{rot}}(1) \times U_{\text{trans}}(1) \rightarrow U_{\text{diagonal}}(1)$.